AD-A042 390 MECHANICAL TECHNOLOGY INC LATHAM N Y F/G 21/5
ADVANCED COMPRESSOR SEAL TESTS.(U)
APR 77 M EUSEPI, L W WINN F33615-75-C-2062
UNCLASSIFIED AFAPL-TR-77-22 NL

| OF |
ADA042390

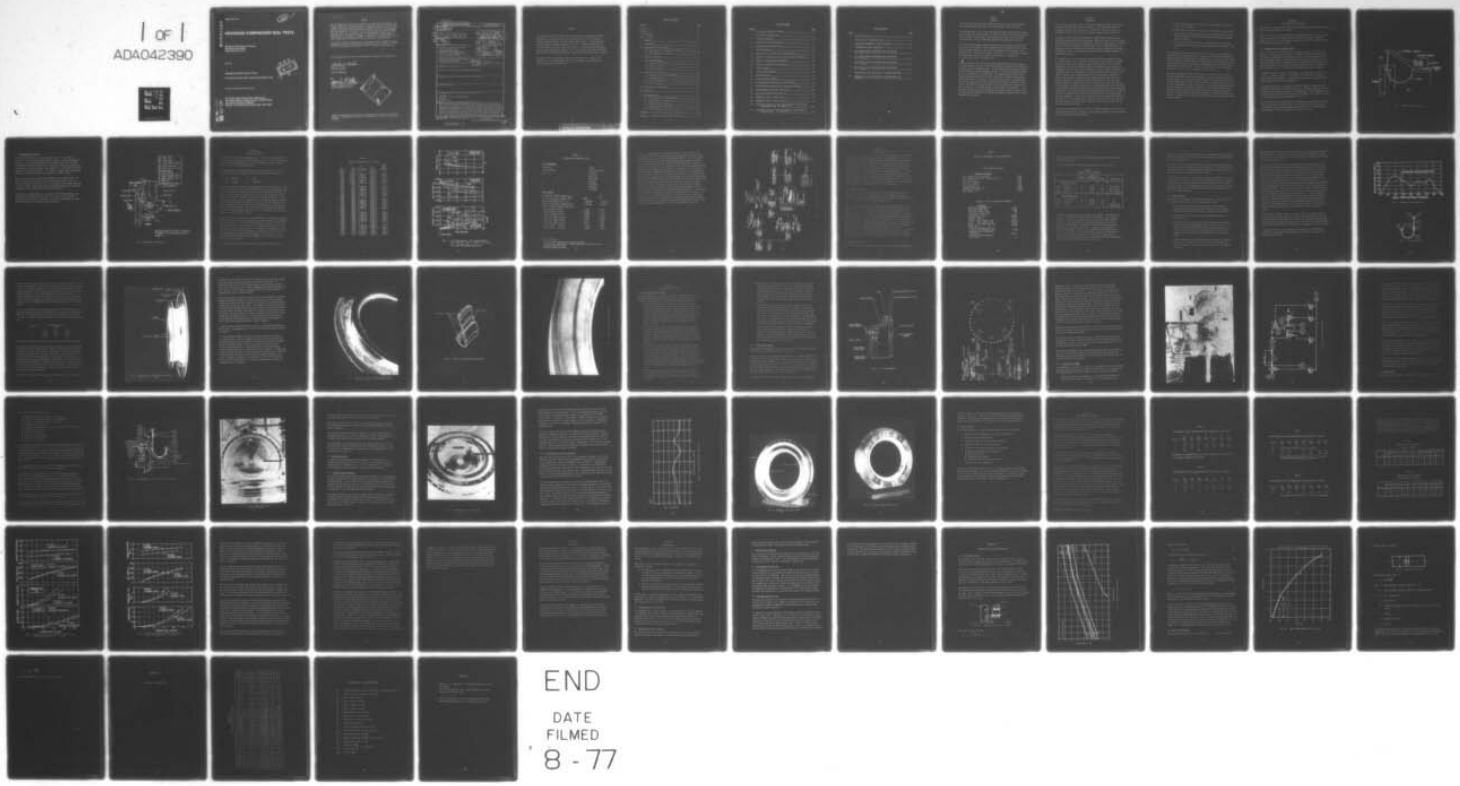

END

DATE
FILMED
8 - 77

AFAPL-TR-77-22

(12)

ADVANCED COMPRESSOR SEAL TESTS

Mechanical Technology Incorporated
968 Albany-Shaker Road
Latham, New York 12110

April 1977

TECHNICAL REPORT AFAPL-TR-77-22

Final Report for Period April 1975 through December 1976

AIR FORCE AERO-PROPULSION LABORATORY
AIR FORCE WRIGHT AERONAUTICAL LABORATORIES
AIR FORCE SYSTEMS COMMAND
WRIGHT—PATTERSON AIR FORCE BASE, OHIO 45433

NOTICE

When Government drawings, specifications, or other data are used for any purpose other than in connection with a definitely related Government procurement operation, the United States Government thereby incurs no responsibility nor any obligation whatsoever; and the fact that the government may have formulated, furnished, or in any way supplied the said drawings, specifications, or other data, is not to be regarded by implication or otherwise as in any manner licensing the holder or any other person or corporation, or conveying any rights or permission to manufacture, use, or sell any patented invention that may in any way be related thereto.

This report has been reviewed by the Information Office, (ASD/OIP) and is releasable to the National Technical Information Service (NTIS). At NTIS, it will be available to the general public, including foreign nations.

This technical report has been reviewed and is approved for publication.

Charles W. Elrod

Charles W. Elrod
Project Engineer

FOR THE COMMANDER

James L. Radloff

JAMES L. RADLOFF, Major, USAF
Chief, Components Branch
Turbine Engine Division

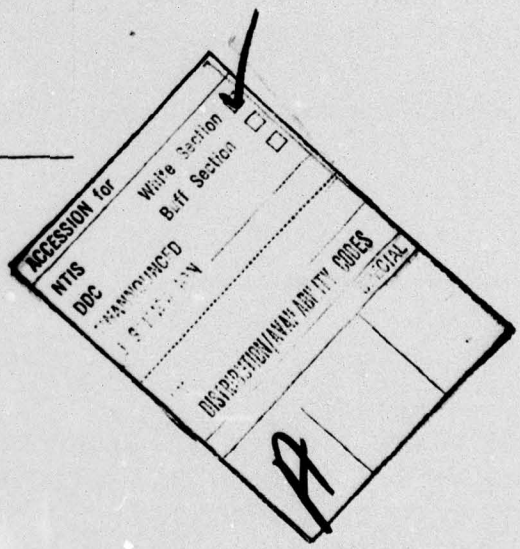

Copies of this report should not be returned unless return is required by security considerations, contractual obligations, or notice on a specific document.

UNCLASSIFIED

SECURITY CLASSIFICATION OF THIS PAGE *(When Data Entered)*

REPORT DOCUMENTATION PAGE	READ INSTRUCTIONS BEFORE COMPLETING FORM
1. REPORT NUMBER: AFAPL-TR-77-22	2. GOVT ACCESSION NO. / 3. RECIPIENT'S CATALOG NUMBER
4. TITLE *(and Subtitle)*: ADVANCED COMPRESSOR SEAL TESTS.	5. TYPE OF REPORT & PERIOD COVERED: April '75 thru December '76 Final Technical Report.
	6. PERFORMING ORG. REPORT NUMBER: Apr 75 - Dec 76
7. AUTHOR(s): M. Eusepi, L. W. Winn	8. CONTRACT OR GRANT NUMBER(s): F33615-75-C-2062
9. PERFORMING ORGANIZATION NAME AND ADDRESS: Mechanical Technology Incorporated, 968 Albany-Shaker Road, Latham, New York 12110	10. PROGRAM ELEMENT, PROJECT, TASK AREA & WORK UNIT NUMBERS: 3066/10/06
11. CONTROLLING OFFICE NAME AND ADDRESS: Air Force Aero-Propulsion Laboratory, Air Force Systems Command, Wright Patterson Air Force Base, Ohio	12. REPORT DATE: April 1977 / 13. NUMBER OF PAGES: 71
14. MONITORING AGENCY NAME & ADDRESS *(if different from Controlling Office)*: Air Force Aero-Propulsion Laboratory, Air Force Systems Command, Wright-Patterson Air Force Base, Ohio	15. SECURITY CLASS. *(of this report)*: Unclassified / 15a. DECLASSIFICATION/DOWNGRADING SCHEDULE

16. DISTRIBUTION STATEMENT *(of this Report)*

Approved for public release; distribution unlimited

17. DISTRIBUTION STATEMENT *(of the abstract entered in Block 20, if different from Report)*

18. SUPPLEMENTARY NOTES

19. KEY WORDS *(Continue on reverse side if necessary and identify by block number)*

Face Seal
Compressor Seal for Turbine Engines
"J" Seal
Compliant Seals

20. ABSTRACT *(Continue on reverse side if necessary and identify by block number)*

The continuation of the development of a new resilient seal concept entitled the "J"-Seal is described. The concept uses a pressure loaded membrane and hydrostatic bearing principles to maintain a minimum stator to rotor clearance Following the development of a complex seal analyses performed in an earlier phase of this program, the seal was built and tested. Seal distortions due to inadequate manufacturing techniques have been substantially reduced through the use of brazing with a high temperature gold alloy instead of welding. The test results presented in this report support the analytically predicted trends

DD FORM 1 JAN 73 1473 EDITION OF 1 NOV 65 IS OBSOLETE

UNCLASSIFIED

SECURITY CLASSIFICATION OF THIS PAGE *(When Data Entered)*

224550 ii

FOREWORD

The program described in this report was conducted by Mechanical Technology Incorporated, Latham, New York, for the United States Air Force Systems Command, Wright-Patterson Air Force Base, Dayton, Ohio. The original phase of this program was under the direction of Mr. J. McCabe, Program Manager. The work described in this report was under Mr. L. Winn's program management. Mr. M. Eusepi was project engineer. Mr. C. W. Elrod of the Flight Propulsion Laboratory at Wright-Pattison Air Force Base was the Air Force Project Manager.

The authors wish to acknowledge the credit due to Mr. H. V. White, the originator of the seal concept, and Dr. A. J. Smalley, who conducted the original analytical investigation.

TABLE OF CONTENTS

LIST OF FIGURES

LIST OF TABLES

SECTION I

SUMMARY

This report discusses the work performed for the Air Force Systems Command, Wright-Patterson Air Force Base, under Contract No. F33615-75-C-2062.

The work described in this report followed the initial analytical and hardware study accomplished under Contract No. F33615-73-C-2043, the objective of which was to develop "clearance type, non-contacting, gas path seals" to replace labyrinth seals in high performance compressors of advanced jet engines.

Under the original program analytical methods for predicting the behavior of the J-Seal were developed. These methods have been incorporated into a step-by-step design procedure by which seal performance can be optimized. The results of this phase of the program are summarized in a final report entitled, "Advanced Compressor Seal for Turbine Engines" by A. J. Smalley and P. R. Albrecht, issued in November 1975.

Within the frame work of the second program phase described in this report, the seal design and the test rig have been modified to permit the incorporation of a more accurate measuring system. A new manufacturing technique involving furnace brazing rather than welding together of the several components making up the seal membrane has been employed. Seal membranes fabricated by this brazing technique although not totally satisfactory, exhibited substantially reduced distortions as compared to earlier welded versions. The improvement of the seal fabrication process permitted the experimental evaluation of the J-Seal. The results of this evaluation produced a qualitative verification of the seal analysis. The prime sealing concept appears to be feasible. As the next step this sealing concept should be incorporated within a realistic face type floating seal design and its dynamic performance evaluated over a range of compressor shaft speeds.

SECTION II
BACKGROUND

Turbine engine compressor seals are important components because they control leakage of the compressor gas and, therefore, are a significant factor in determining overall engine efficiency. Because of current fuel costs and availability alone, the efficiency of advanced engines must be maximized.

In general, seal technology development has lagged behind compressor aerodynamics technology because the aerodynamic analytical models are sophisticated and augmented with empiricism from carefully controlled measurements. Currently, there is a much more promising probability to achieve a significant gain in engine efficiency by improving seal performance than by improving aerodynamic performance. This is the reason why the subject seal technology program is so important and timely.

The labyrinth seal is the design most often utilized for compressor sealing. As a single stage device, labyrinth seals have been used to obtain reasonable engine efficiency, up to a pressure differential of about 50 psi, with gas temperatures in the neighborhood of 500°F. When buffered by introducing an intermediate pressure gas, and multi-staged in steps of different diameter, the performance range of a labyrinth seal system has been extended to 400 psi and 1200°F. However, these configurations are relatively heavy, expensive to machine and difficult to install without damage to their sharp knife edges. In most instances the labyrinth seal will rub against the bore requiring special materials to assure proper rubbing compatibility. As a side product of the rubbing, the sharp knife edges may get worn down and/or pick up material, thus disturbing the engine balance which in some instances may have disasterous consequences. No doubt the efficiency of labyrinth seal systems can be improved with the development effort that is currently going on in most engine manufacturing companies. However, the configuration of these systems is heading in the direction of increased complexity and the original features that made the labyrinth attractive, namely high reliability, long life, and simplicity are gradually being eroded away.

A concept evaluated under contract F33615-73-C-2043 suggested a new compressor sealing approach based on compliance. The proposed compliant seal was conceived in view of the following requirements:

- A close clearance seal is required to avoid compressor efficiency losses due to leakage.
- A face seal configuration is necessary to accommodate radial growth.
- The seal face of a close clearance seal must comply with distortions arising both from manufacturing tolerances and operational induced geometric changes.
- The mass of the seal member must be minimized in order to permit tracking of the varying axial position along the circumference of the seal.

The minimum mass compliant structure to carry the seal face and separate the high from the low pressure areas is a membrane. The minimum mass membrane that can support a seal dam from the engine stator is a circular cross section toroid with the outer half removed and replaced by a direct connection to the housing on one side and a thin washer type connection from the seal down to the housing on the other side. Because its curved cross-section resembles the letter "J", this seal is referred to as the "J-Seal".

An analytical parametric study of the J-Seal was performed and a 13-inch diameter compressor seal has been designed to operate at 600 psi and 1500°F. A seal and seal test rig have been constructed for initial verification tests at room temperature and at 100 psi air pressures. A detailed description of the work accomplished is given in Reference 1. This report describes the test results obtained in the follow-on phase of the J-Seal development in which test data was obtained that qualitatively verifies analytically predicted behavior of some of the more important parameters. Further work however, is required to broaden the test range and obtain qualitative verification between test and analyses.

SECTION III

DESCRIPTION OF SEAL CONCEPT

The J-Seal is a face type seal capable of accommodating large axial excursions as well as radial whirl of the shaft.

The seal version used in this program is representative of the primary sealing surfaces only, while the finished seal version will eventually comprise a floating seal body. The differences between the test and final seal versions are described in more detail below.

3.1 Description of a Jet Engine J-Seal

A final version of a jet engine J-Seal is shown in Figure 1. The seal consists of a runner which is mounted on the shaft and operates at shaft speed. The runner is equipped with a seal face located at its outer diameter. The face is slightly tapered to provide convergent flow during operation. It is this convergence which is responsible for the bearing type action of the seal during operation and the inherent stiffness resulting from it is employed to keep the runner at a safe but minute film distance away from the stator.

The stator is built into the J-Seal membrane. Its dimensions are defined by r_o and r_i as shown in Figure 1. The membrane is welded onto a secondary carrier which is subjected to a constant preload by a set of springs equally spaced around the full seal circumference.

The high pressure P_{HI} is located on the outside diameter of the runner and is thus also present in the preload spring area. The fact that the seal has to maintain axial floating capability is responsible for the introduction of a secondary seal, usually a piston ring, which is placed in the stator and forms a circumferential ring type seal with the carrier.

Since one of the prime objectives of this program was to validate the analytical calculations, the seal used on test was simplified in the sense that the primary seal face was fully duplicated, but the axial flotation feature was eliminated in order to render the testing more economical.

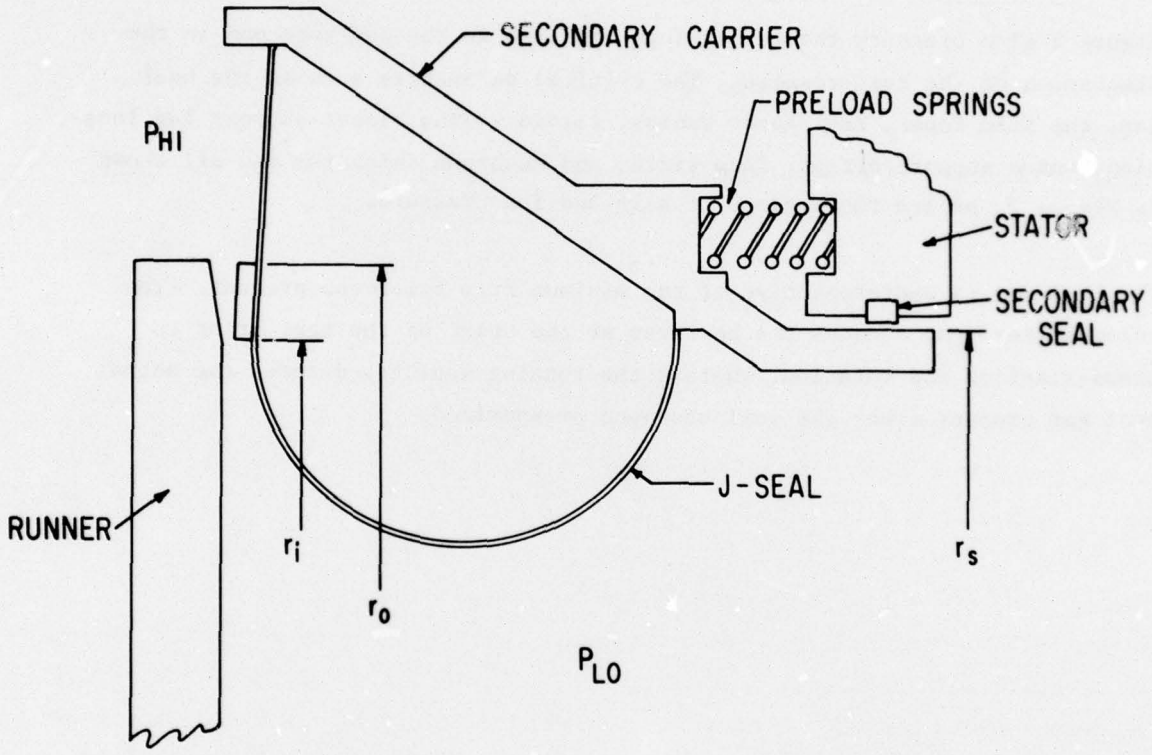

Fig. 1 Jet Engine Compressor "J-Seal"

3.2 Description of Test Seal

A cross-section of the test seal is shown in Figure 2. The runner is similar to the runner which would be normally used in a final sealing application, as is the J-Seal membrane and the stationary seal ring. The only substantial difference between the test seal and an eventual jet engine seal version lies in the fact that the J-Seal membrane is, in this particular case, attached to a stationary support. In an actual jet engine seal, as explained before, the membrane would have been attached to a movable carrier.

Figure 2 also presents the terminology employed in the analyses and in the discussion of the test results. The critical parameters such as the heel gap, the film taper, seal inner radius, toroid radius, inner support leg location, outer support offset, face width, and membrane thickness are all shown in Figure 2, as are the regions of high and low pressure.

The heel gap is representative of the minimum film thickness present. The unloaded heel gap denotes the heel gap at the start of the test prior to pressurization and rotation, whereas the running heel gap denotes the actual heel gap present after the seal has been pressurized.

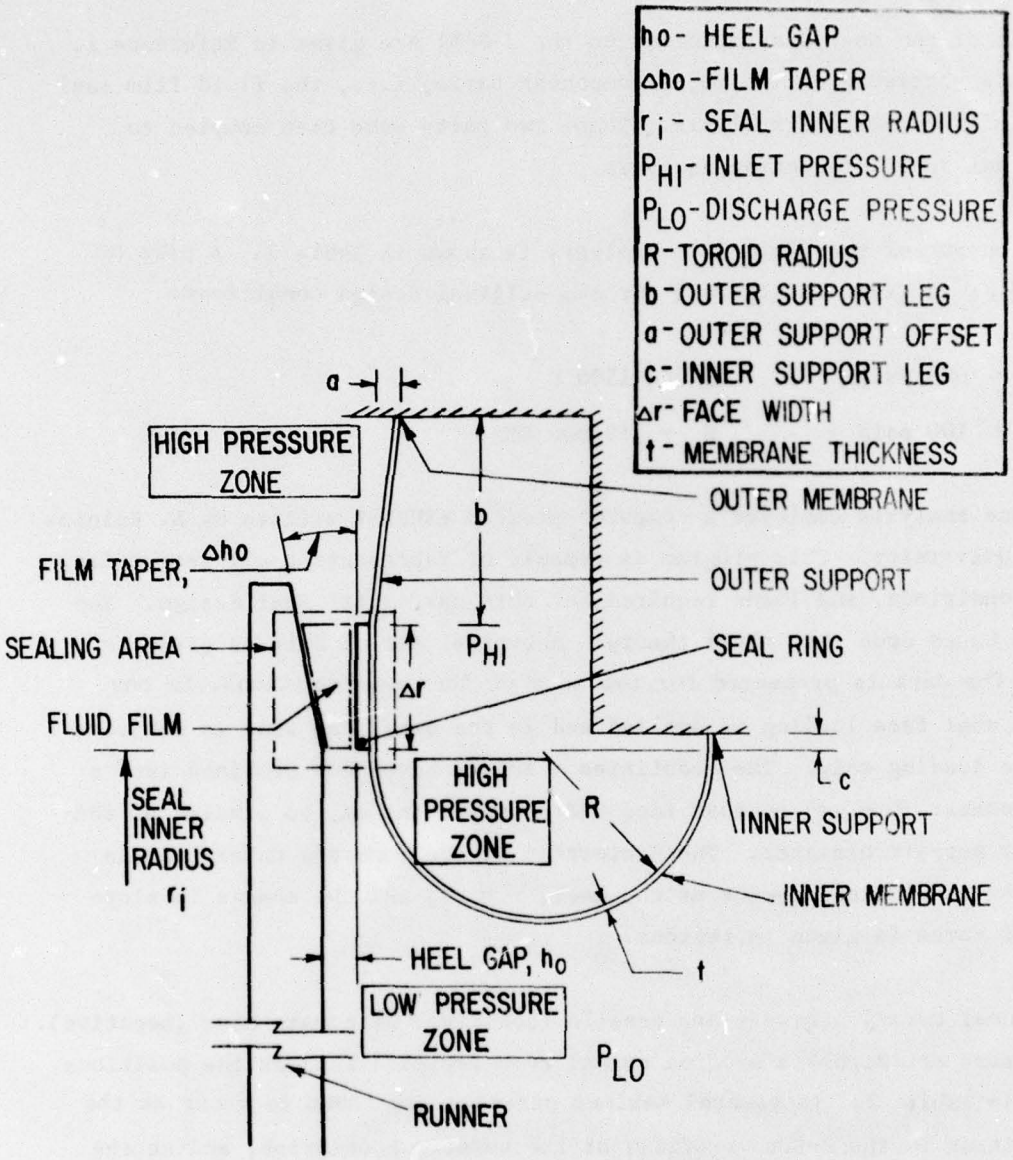

NOTE: FILM TAPER IS EXPRESSED THROUGHOUT IN TERMS OF THE DIFFERERENCE IN GAP AT OD AND ID

Fig. 2 The J-Seal – Nomenclature

SECTION IV
REVIEW OF ANALYSIS

The details of the analysis performed on the J-Seal are given in Reference 1. The analysis consisted of two major component parts, i.e., the fluid film seal analysis and the membrane analysis. These two parts were then coupled to yield a final seal interaction analysis.

A typical output of the fluid film analysis is shown in Table 1. A plot of the variables in given in Figure 3 for the original design conditions:

P_{HI} = 600 psig T = 1500 F

P_{LO} = 100 psig N = 12,000 RPM

The membrane analysis employed a computer program KSHEL-1 written by A. Kalnins of Lehigh University. This program is capable of representing all geometries, boundary conditions, and loads required for this particular seal design. The program is based upon thin shell theory. A typical set of data is given in Table 2. The data is presented for two sets of loading conditions, in one set a pure seal face loading is applied and in the other the seal is subjected to pressure loading only. The quantities b and Δr have been combined into a single parameter $(b + \Delta r)$ so that face width variations may be studied at constant outer support diameter. The distortion of the membrane under load is given as the axial displacement at the heel, $r = r_i$, and the change in slope of the seal force is given in radians.

The meridional normal stresses are tensile (positive) or compressive (negative). These stresses act across a section normal to a meridian line at the positions indicated in Table 2. In general maximum stresses are found to occur at the discontinuities in the J-Seal profile: at the support boundaries, and at the inner and outer edges of the seal face. The coupled seal analysis, from here on referred to as the interaction analysis, was written to carry out the overall seal calculations which include the appropriate interpolations. The interaction analysis program is given in Appendix B of Reference 1 together with the input designations.

The methodology of the seal design process is shown in the flow chart in

TABLE 1

FLUID FILM DATA FOR Δr = 0.75 IN.

h_o (IN)	Δh_o (IN)	Q_L (LB.SEC/IN)	F_F (LB)	POWER LOSS (WATTS)
0.0000	0.0000	0.	16198.0	∞
.0005	0.0000	3.278E-05	10347.0	4998.0
.0010	0.0000	1.896E-04	10335.0	3417.0
.0020	0.0000	7.679E-04	10332.0	2569.0
.0030	0.0000	1.631E-03	10320.0	2244.0
.0040	0.0000	2.800E-03	10309.0	2030.0
.0050	0.0000	4.130E-03	10262.0	1868.0
0.0000	.0020	0.	16198.0	∞
.0005	.0020	1.935E-04	14215.0	3468.0
.0010	.0020	5.169E-05	13384.0	2953.0
.0020	.0020	1.388E-03	12461.0	2435.0
.0030	.0020	2.532E-03	11963.0	2154.0
.0040	.0020	4.000E-03	11650.0	2020.0
.0050	.0020	5.426E-03	11456.0	1899.0
0.0000	.0040	0.	16198.0	∞
.0005	.0040	3.255E-04	14792.0	2982.0
.0010	.0040	7.806E-04	14220.0	2662.0
.0020	.0040	1.909E-03	13390.0	2320.0
.0030	.0040	3.317E-03	12849.0	2130.0
.0040	.0040	4.850E-03	12450.0	2010.0
.0050	.0040	6.591E-03	12191.0	1903.0
0.0000	.0080	0.	16198.0	∞
.0005	.0080	5.995E-04	15105.0	2568.0
.0010	.0080	1.238E-03	14795.0	2406.0
.0020	.0080	2.816E-03	14222.0	2198.0
.0030	.0080	4.591E-03	13766.0	2056.0
.0040	.0080	6.533E-03	13397.0	1948.0
.0050	.0080	8.500E-03	13020.0	1850.0
0.0000	.0120	0.	16198.0	∞
.0005	.0120	9.139E-04	15203.0	2342.0
.0010	.0120	1.700E-03	15004.0	2234.0
.0020	.0120	3.617E-03	13596.0	2084.0
.0030	.0120	5.714E-03	14227.0	1974.0
.0040	.0120	8.012E-03	13908.0	1888.0
.0050	.0120	1.320E-02	13660.0	1790.0

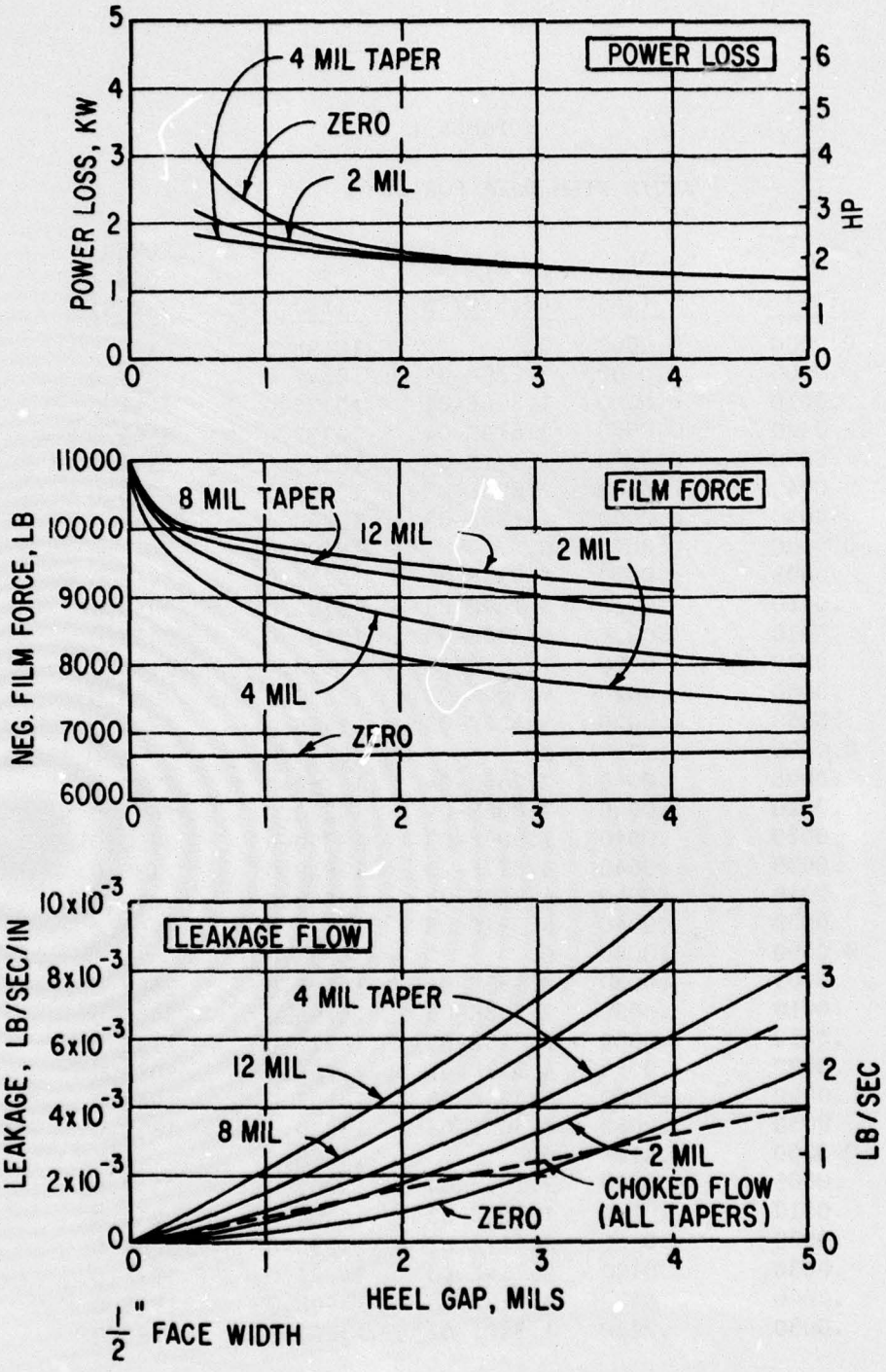

Fig. 3 J-Seal Performance - 1/2 Inch Face Width; P_{HI} = 600; P_{LO} = 100, T = 1500 F, ID = 13 In., N = 12,000 RPM (Design Conditions)

TABLE 2

TYPICAL SET OF FLEXIBILITY DATA

INPUT PARAMETERS

Temperature	1500°F
Young's Modulus	20.0×10^6 lb/in^2
(b + Δr)	2.00 inch
c	0.067 inch
t	0.045 inch
r	6.5 inch
Δr	0.50 inch
a	0.00 inch
R	1.00 inch

OUTPUT RESULTS

ΔP, Membrane Pressure Loading, psi	0	500
F_N, Total Seal Force Loading, lbs.**	1000	0
Axial Displacement*, inch, at r	- .0058769	- .0043181
Change in Face Slope*, radians (psi)	- .0037515	+ .0014411
Meridional Normal Stresses* (psi) at:		
Outer support (inside)	- 11036	+ 4624
Outer support (outside)	+ 12092	+ 11727
Outer face edge (inside)	+ 16029	+ 12550
Outer face edge (outside)	+ 14797	+ 6528
Inner face edge (inside)	+ 9787	+ 16081
Inner face edge (outside)	- 8435	+ 4847
Inner support (inside)	+ 15178	+ 8903
Inner support (outside)	- 13928	+ 12436

*Sign Conventions:

Positive axial displacement is away from runner
Positive face slope induces a converging film in direction of flow
Positive stress is tensile

**Positive toward the runner

Figure 4. Starting with the rectangular enclosure on the left-hand side on the upper part of the rectangle, the fluid film analysis is located which generates the data for the fluid film performance tables. On the lower part of the rectangle we see the thin shell analysis which generates the data of stress and seal flexibility. The environment conditions such as pressure, temperature, and speed are used as inputs into the interaction analysis program together with the seal geometric parameters. The output of the interaction analysis produces leakage, running heel gap, and power vs. the unloaded heel gap and its taper. Once a set of limiting values related to the maximum flow and permissible stress, as well as the optimum taper and running heel gap limitations, have been established the data when plotted can take these limited values into account and produce finite barriers within which the seal performance would be acceptable. An example of such a plot is also shown in Figure 4. This plot, in turn, can serve as a means for selecting the proper values of film taper and heel gap which will yield acceptable performance. In order, however, to finalize the geometry anticipated, uncertainties in the unloaded film taper must be considered together with the effects of thermal distortion at running conditions. For the purposes of this program the effect of thermal distortion was assumed to be minimal because of the stationary nature of tests which were subsequently performed to verify the analytical predictions.

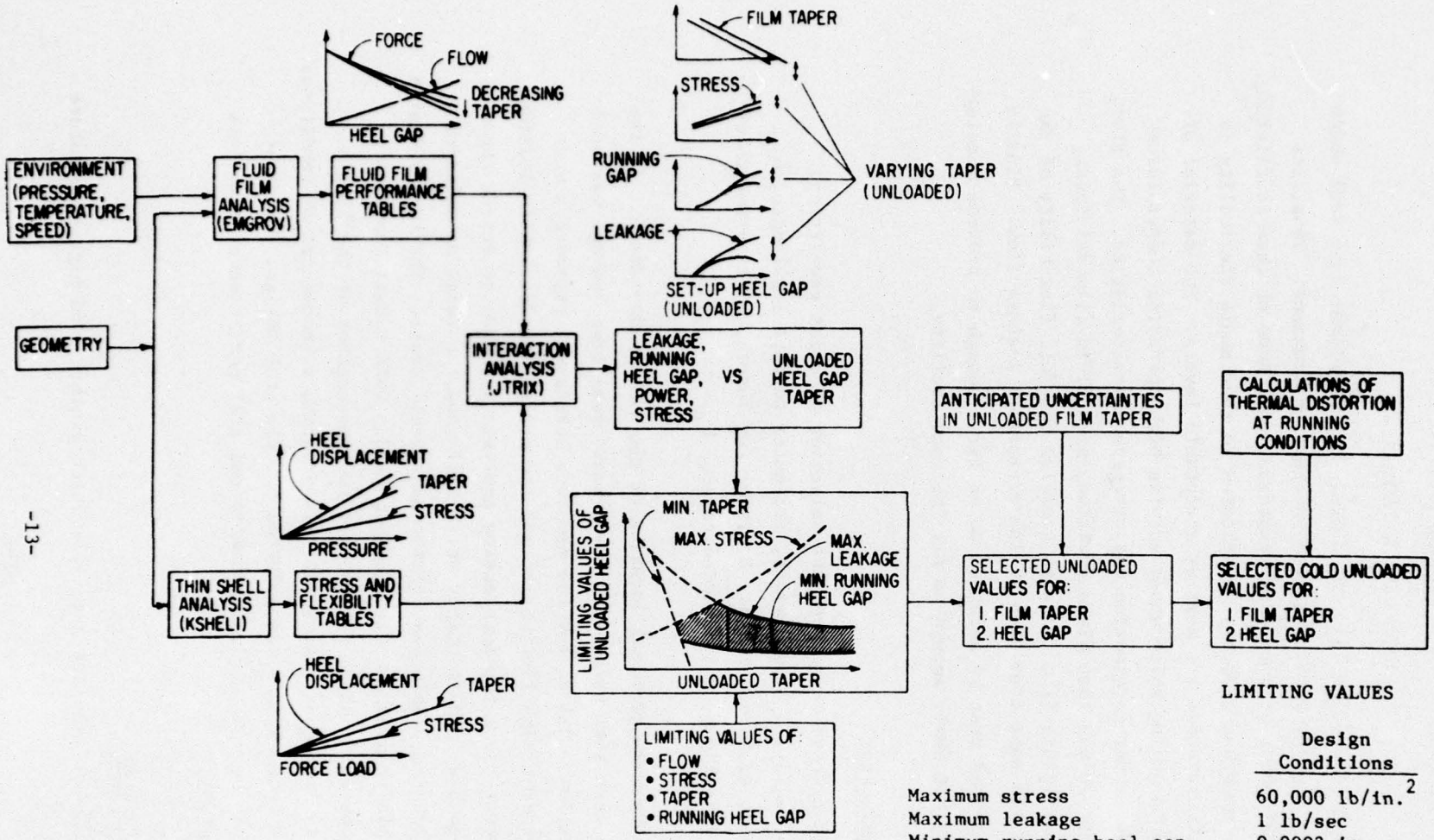

LIMITING VALUES

	Design Conditions
Maximum stress	60,000 lb/in.^{2}
Maximum leakage	1 lb/sec
Minimum running heel gap	0.0002 in.
Minimum running film taper	0.003 in.*
Pressure, Psi	600
Temperature, °F	1500

Fig. 4 Flow Chart for J-Seal Analyses

SECTION V

SEAL DESIGN SUMMARY

As was pointed out in Section III, the J-Seal is a compliant face seal which must operate in a high temperature, high pressure environment. Thus, its design involves a number of important considerations, some of them conflicting. For example, the membrane geometry is selected so that ample flexibility is provided while the stresses are kept at acceptable levels. The material of construction has to be one which would survive high operating temperatures and still provide proper deformation and strength characteristics. The fluid film geometry must be one that gives positive, high fluid film stiffness, sufficient range of fluid film force to exercise the full flexibility of the membrane, and at the same time also yields acceptable leakage flow. Finally, the size of the J-Seal must be selected to be large enough to provide meaningful test results, but small enough to fit the test facility.

5.1 Parameter Selection

The J-Seal design process considered the selection of eight geometrical parameters: seal radius, r_i; face width, Δr; outer support leg length, b; outer axial offset, a; toroid radius, R; inner leg length, c; membrane thickness, t; unloaded heel gap, h ; unloaded taper, h_∞.

Figure 2 illustrates the physical location of the listed parameters. In the selection of the test seal parameters the primary seal face leakage was used as the main criterion. Values for the membrane structural parameters were synthesized to provide high flexibility and low stress sensitivity to loading. With these parameters set, the interaction analysis was used to select those values of unloaded heel gap and taper which maximized the range of unloaded heel gap over which acceptable seal performance would occur. The target design conditions for this program are given in Figure 3. This target represents a set of conditions anticipated in advanced turbine engines of the 1980's. Recognizing the developmental nature of this program, a second set of conditions typical of nearer term engines was selected for the seal design. The test design conditions, the seal minimal geometry and seal performance parameters are listed in Table 3.

5.2 Material Selection

The present application requires materials which exhibit good high temperature

TABLE 3

PREDICTED PERFORMANCE AT TEST CONDITIONS

J-SEAL NOMINAL GEOMETRY

Dimension (inches)	
Outer support axial offset, a	0.00
Outer leg length and face width (b + Δr)	2.00
Face width, Δr	0.75
Membrane thickness, t	0.03
Inner leg length, c	0.10
Toroid radius, R	1.00
Unloaded film taper, Δh_{∞}	0.005
Unloaded heel gap, h_{∞}	0.013
Seal radius, γ_i	13.00

SUMMARY OF J-SEAL PERFORMANCE PARAMETERS

Parameter	
Operating temperature, F	1,200
Operating speed, rpm	12,000
Upstream pressure, psi	300
Discharge pressure, psi	50
Running heel gap, in.	0.0014
Running taper, in.	0.0073
Leakage, lb/sec	0.21
Stress - outer support, psi	19,400
Stress - inner support, psi	25,700
Stress - outer face edge, psi	18,600
Power, hp	2.3
Stress fluctuation (psi) for 4 mil runout (peak-to-peak)	9,700
Leakage per unit perimeter, lb/sec/in.	0.0051
Allowable range of unloaded gap, mils	± 5

stability, good resistance to oxidation corrosion, high yield stress, and good forming characteristics.

A list of materials with these required properties is given in Table 4.

TABLE 4

J-MEMBRANE MATERIAL CANDIDATES

		MACHIN-ABILITY	YIELD STRENGTH PSI (.2% OFFSET)	MODULUS	STOCK FORM
	1500°F Temperature				
Ni-46	Waspalloy	.12	73,000	22.7	Bars, Sheets
Ni-97	Hastelloy R-235	~.10	59,000	18.8	Bars, Sheets
Ni-28	Udimet 500	.09	100,000	23.4	Bars, Forgings
	1200°F Temperature				
Ni-115	Inconel X750	.15	120,000	31.0	All
Ni-179	Inconel 617	~.10	135,000	NA	All
Ni-47	René 41	.15	116,000	25.9	Sheets, Bars Rates, Flat

The 1500^{O}F materials would perform adequately at 1200^{O}F but are generally more expensive, less available and more difficult to fabricate. Cost and availability are important considerations, particularly for the 1500^{O}F condition where only a very limited range of stock sheet is available. The final material selected from Table 4 as being suitable for the test program were Waspalloy and Inconel X-750, respectively. Hastelloy, R-235 and Rene 41 offered slightly higher retention of stress properties and physical characteristics at their respective elevated temperatures, but were discounted due to their high cost and limited availability in sheet form. Udimet 500 and Inconel 617 were adequate with respect to strength and temperature requirements, but generally less available in the smaller sheet form.

Composite materials were considered and they may eventually be good candidates for future evaluation. However, they do not presently hold near term promise for J-Seal applications.

The final selection of Inconel X-750 as the seal membrane material was based on the selection of the 1200°F seal design temperature. The added expense of fabricating the seal from Waspalloy when a 1500°F test condition was not planned for the advanced test phase was not warranted.

Subsequent to the award of this contract, the government-supplied air supply system that was scheduled to be used on this program was no longer available; a redefinition of the test temperature was made, reducing it from 1200°F to 100°F. Although the test temperature was reduced, no modification to selected seal material was made, thereby maintaining the fabricated membrane's suitability for 1200°F operation.

5.3 Seal Fabrication

The original J-Seal membrane was fabricated from 20 to 22 gauge (0.040 in. thick) Inconel X-750 sheet stock by the following technique:

a) A rectangular sheet of material was rolled to form a cylinder having a diameter equal to the minimum diameter of the completed membrane and with sufficient length to provide spinning material.

b) The seam of the cylinder was joined by Tungsten Arc-inert gas (TIG) welding.

c) With appropriate tooling each end of the cylinder was spun radially outward in an arc; spinning both cylinder ends in a 90° arc, a toroidal section having a 180° arc length and proper diameter was formed. The movement caused by the spinning process reduced the membrane thickness to 0.035 in. at the free ends of the partial toroid.

d) A washer shaped disc of Inconel X-750, cut to fit both the diameter of one leg of the partial toroids open side and of the housing mount, was then TIG butt welded to the toroid to form the complete J-membrane.

This manufacturing method was recommended by the spin-forming vendor as having the best chance of success based on his experience with spinning high temperature materials. Any distortions caused by welding were expected to be removed by the spinning process.

The weld which was made to form the toroidal section was planished and cold worked during the spinning operation and caused no distortions. The weld of the leg, however, was in a location where cold working could not be performed and extensive distortions on this part resulted from the weld and remained present even after several attempts at planishing. In this area (the same location as the attachment point of the seal dam) these distortions caused severe lack of parallelism between the seal dam and the seal runner. In an attempt to reduce the waviness of the membrane the long support leg was slotted with 32 equally spaced radial slots 3/16" wide and 1-11/16" long starting at the outside diameter. This slotting considerably reduced the membrane waviness in the seal area expecially when retained in the test fixture. The resulting seal dam distortions, however, were not eliminated. It can be clearly seen in Figure 5 that the maximum distortion is still many times larger than the expected setup and running heel gap. These distortions subsequently proved too large to permit the extraction of any meaningful data from early test results. It became apparent after the initial tests that an alternate manufacturing method was required in order to obtain a membrane suitable for testing.

The fabrication technique which was selected as the most promising presents a variation of the earlier procedure. The toroidal section and the long leg of the J-membrane are fabricated as initially. The disc and toroid are then furnace brazed to an especially machined seal dam to form the complete membrane. The brazing technique, however, did require some redesign of the seal membrane.

In the new design the J-Seal membrane is an assembly of eight individual components. Schematically these components are identified on Figure 6 and are described as follows.

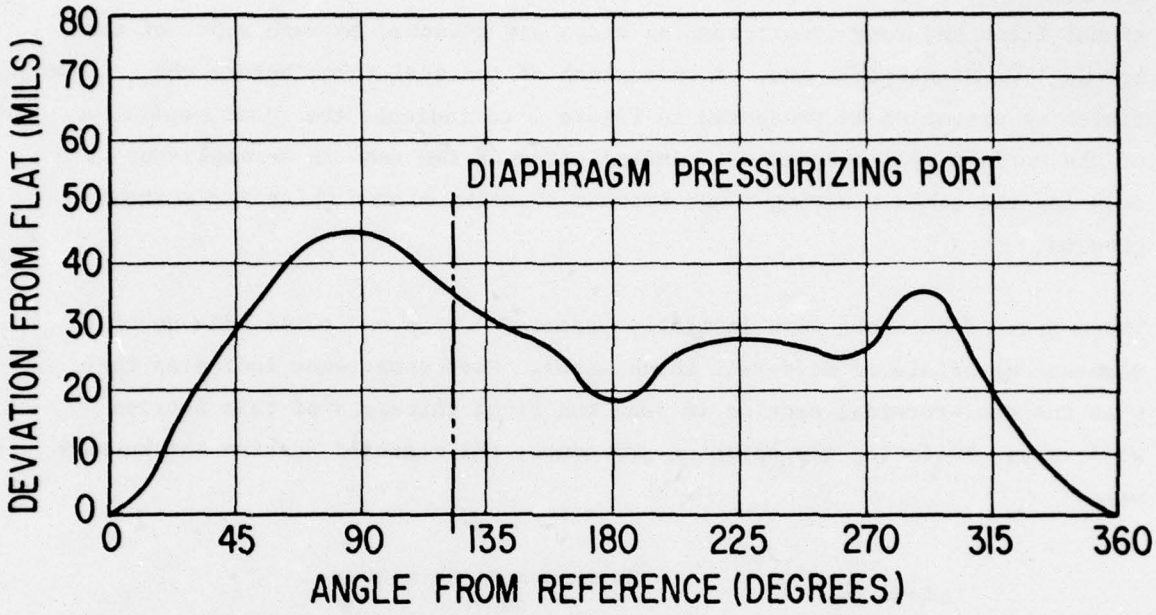

Fig. 5 Original Seal Dam Distortion

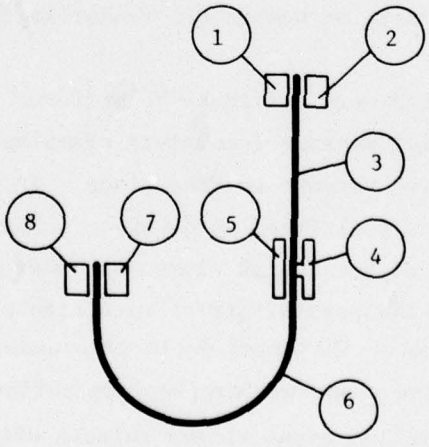

Fig. 6 "J" Seal Components

The front and rear outer clamping ring 1 and 2 are situated on either side of the support diaphragm 3. The static seal runner 4 and the seal runner coupling 5 connect the support diaphragm 3 to the toroidal membrane section 4. Additional front and rear inner clamping rings are attached to both sides of the toroidal membranes free end. A photograph of the seal taken before the finishing operation is presented in Figure 7 to indicate the final positions of the various seal components. Installation of the seal is accomplished by securing the seals clamping rings between mounting plates which are suitably grooved.

Three sets of hardware were initially prepared - each set to be made up of membrane materials of different thicknesses. Past experience indicated that when the semi-toroidal section is spun the final thickness of this section will vary. Following the spinning procedure, the measured section thicknesses were:

Seal No.	Thickness at Section inches		
	3	4-5	6
1	0.043	0.199	0.035
2	0.031	0.187	0.025
3	0.025	0.181	0.020

For identification of the section number the reader is referred to Figure 6.

The brazing operation proved very difficult to perform. The initial attempts at brazing were unsuccessful because incomplete clamping of all the membrane elements permitted excessive warpage to take place. In addition to excessive warpage which distorted the seal face, voids where no braze material was evident developed between adjacent seal elements. Where these voids occurred at the static seal runner the possibility of machining a true seal face on the brazed assembly became remote. Material deflection under the tool load at the void locations would produce a non-uniform sealing surface. The existence of the voids could furthermore introduce stress raisers which could result in seal destruction during operation.

The method of filling the voids that was initially selected utilized a low

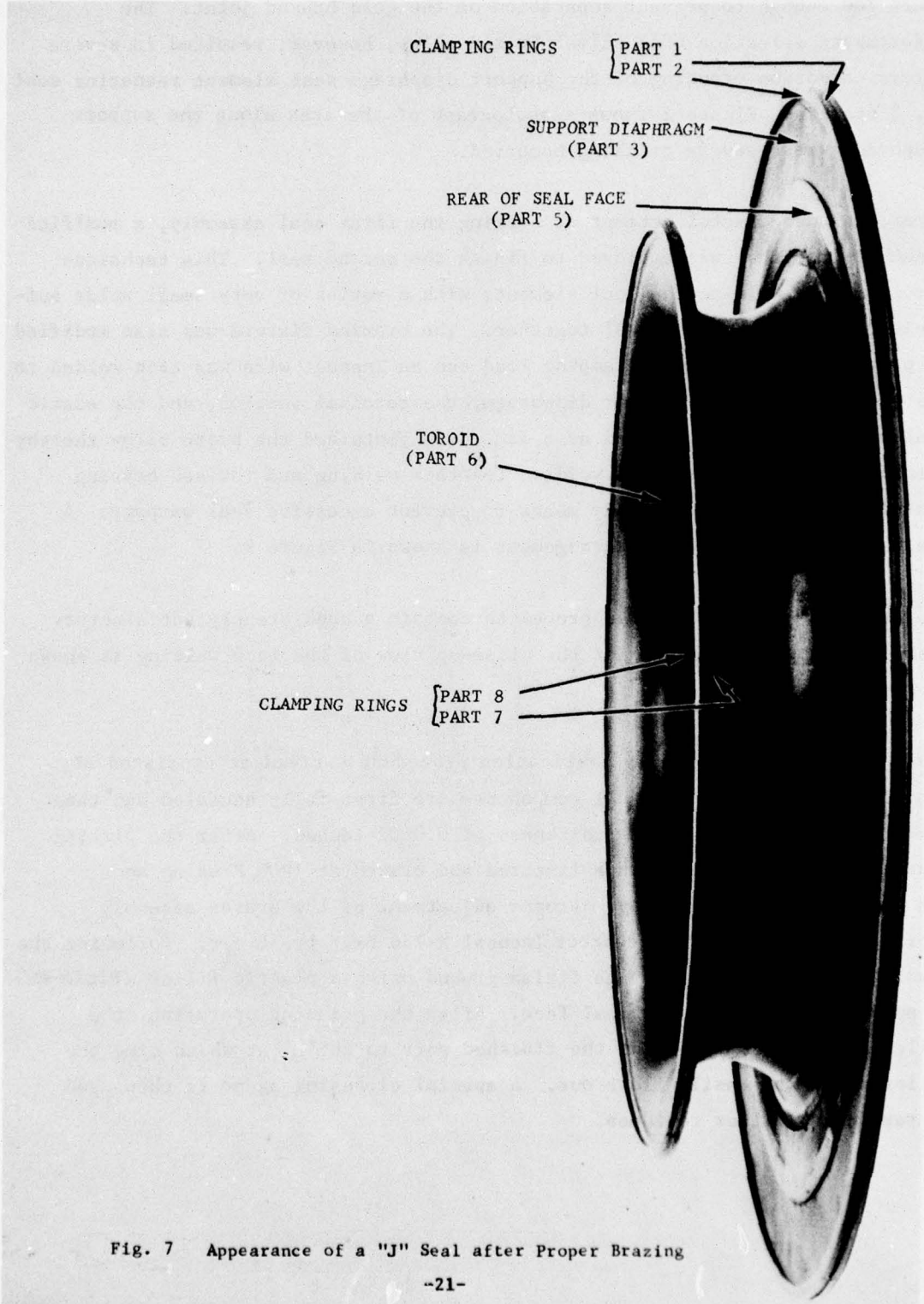

Fig. 7 Appearance of a "J" Seal after Proper Brazing

melting point braze material which could be flowed into the voids at a temperature low enough to prevent separation of the gold brazed joint. The unfortunate selection of a silver brazed alloy, however, resulted in severe stress corrosion cracking of the support diaphragm seal element rendering seal No. 3 useless. Figure 8 shows a photograph of the area along the support diaphragm where severe cracking occurred.

After the unsuccessful attempt at brazing the first seal assembly, a modified assembly technique was employed to finish the second seal. This technique involved tack welding the seal elements with a series of very small welds sufficient only to hold the seal together. The brazing fixture was also modified to provide a more uniform clamping load and an Inconel wire was tack welded to the joint between the support diaphragm, the toroidal section, and the static seal runner. The wire served as a dam which contained the braze alloy thereby eliminating the formation of voids. The tack welding and revised brazing fixture provided the necessary means to prevent excessive seal warpage. A sketch of the tack welding arrangement is shown in Figure 9.

The seal assembly as received proved to contain a consistently satisfactory brazed joint. A photograph of the close-up view of the tack welding is shown in Figure 10.

The final membrane assembly fabrication procedure arrived at consisted of the following steps. The seal components are first fully annealed and then electroless nickel plated to thickness of 0.0002 inches. After the plating process the membrane parts are fixtured and brazed at 1800 F using an 82% Au- 18% Ni brazing alloy. Proper adjustment of the brazed assembly cooling rate provides the correct Inconel X-750 heat treatment. Following the brazing cycle the seal face is finish ground using a plastic filler (Rigid-ex) to provide support for the seal face. After the grinding operation, the filler is removed by heating the finished part to 265°F, at which time the filler melts and easily flows out. A special cleansing agent is then used to remove any filler residues.

Fig. 8 "Seal No. 3 - Effects of Silver Braze Alloy on Inconel" (Note severe stress corrosion cracking)

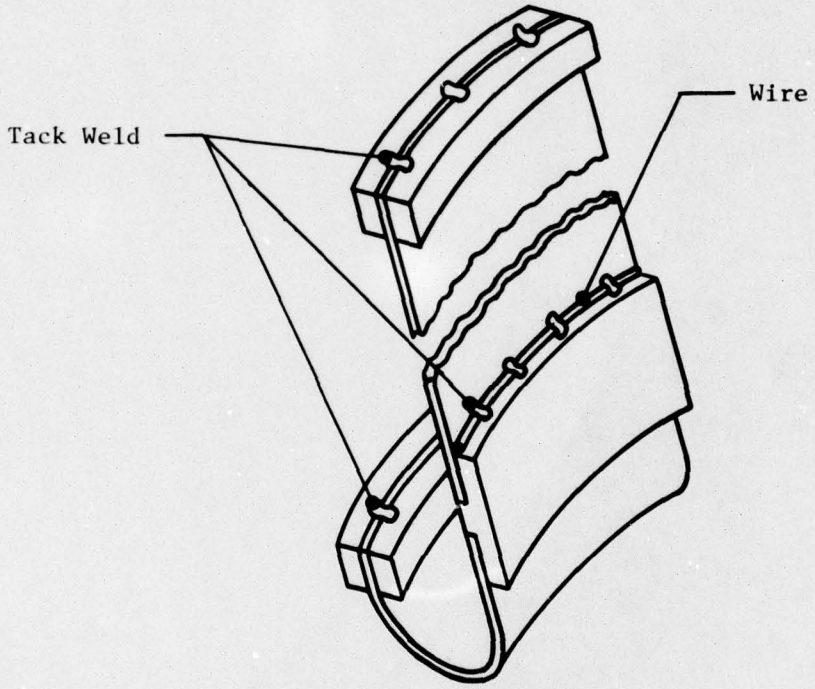

Fig. 9 Sketch of Tack-Welding Arrangement

Fig. 10 Close-up View of Inconel Wire Tack-Weld

SECTION VI

DESCRIPTION OF TEST RIG

6.1 Modification of Tester Hardware

A detailed examination of the previous J-Seal test configuration led to the conclusion that several critical modifications to both the test vehicle and to its installation were necessary. Included in these modifications were:

- The design of a differential bolting system to accurately adjust the test seal's heel-gap settings. Prior to this modification it was necessary to reposition the entire rotating assembly including the seal runner and the drive spindle to change a heel-gap. The new bolting system permitted the heel-gap adjustment to be made by moving the non-rotating seal rather than the entire rotating assembly. A revised sealing method employing large cross section O-Rings was used to maintain an airtight housing at any adjusted position of the seal housing.

- Relocating the test vehicle onto a substantial structural iron test stand combined with a 100 hp variable speed drive. To accomplish this move, an existing machine base was modified to accept the large test seal housing. The new base for the tester provided the rigid foundation required for performing the dynamic test program. The new drive permitted precise speed control up to the maximum test speed of 12,000 rpm.

- The addition of a large air receiver and a seal-air filter in order to provide seal air of sufficient quality for test purposes. The use of an oil lubricated, piston-type boost compressor to supply more high pressure seal air had the propensity of adding two unwanted variables to the test program; pulsations in the supply pressure resulting from piston stroking and oil vapor caused by oil blow-by at the compressor's piston rings. An air receiver with a 100 ft^3 displaced volume and a high pressure oil separator were added to the seal air supply circuit to eliminate both the supply air pulsations and the oil vapor.

- The redesign of the load balancing piston labyrinth to provide two-piece replacement for the one piece seal previously used. The original seal could not be removed without completely disassembling the tester.

- The addition of a static seal runner to allow the use of position measuring instrumentation for direct seal clearance measurements during non-rotating tests. The new static seal runner duplicated all the important dynamic seal runner dimensions, but included two position sensors in each of two orthogonal locations at the seal interface. The two-position sensors at each location were displaced radially to permit determination of possible seal face rotation.

- The redesign of the seal membrane holding arrangement which was necessitated by the redesign of the seal membrane. The original method of securing the seal membrane to the tester housing required welding the thin seal membrane to substantial mounting rings which were in turn to be bolted to the main seal support. Welding experience incurred during the earlier seal fabrication showed that it was not possible to perform the type of welding required by the original seal mounting technique without severely distorting the membrane.

  The redesign of the seal membrane, directed to improve manufacturability, included the addition of clamping rings to both the innermost and outermost mounting locations (see Section 3.2 of this report). In order to accommodate the new clamping rings built into the seal membrane, mounting grooves were added to all the inner and outer mounting rings of the J-Seal holder.

6.1.2 Seal Tester Assembly

The internal configuration of the Seal Tester Assembly including its necessary modifications is illustrated by Figures 11 and 12.

Figure 11 shows the J-Seal membrane assembled into its holder. Identified on the figure is the J-Seal membrane assembly, the J-Seal holder and both the diaphragm and toroid support rings. Included in the assembly is a shim which is used to position the seal's active face at its proper location relative to the seal holder mounting surface. The circumferential thickness of the shim was also adjusted by means of local shim additions in order to minimize the circumferential runout of the test seal's active face.

The complete Seal Tester Assembly is shown in Figure 12. In this assembly

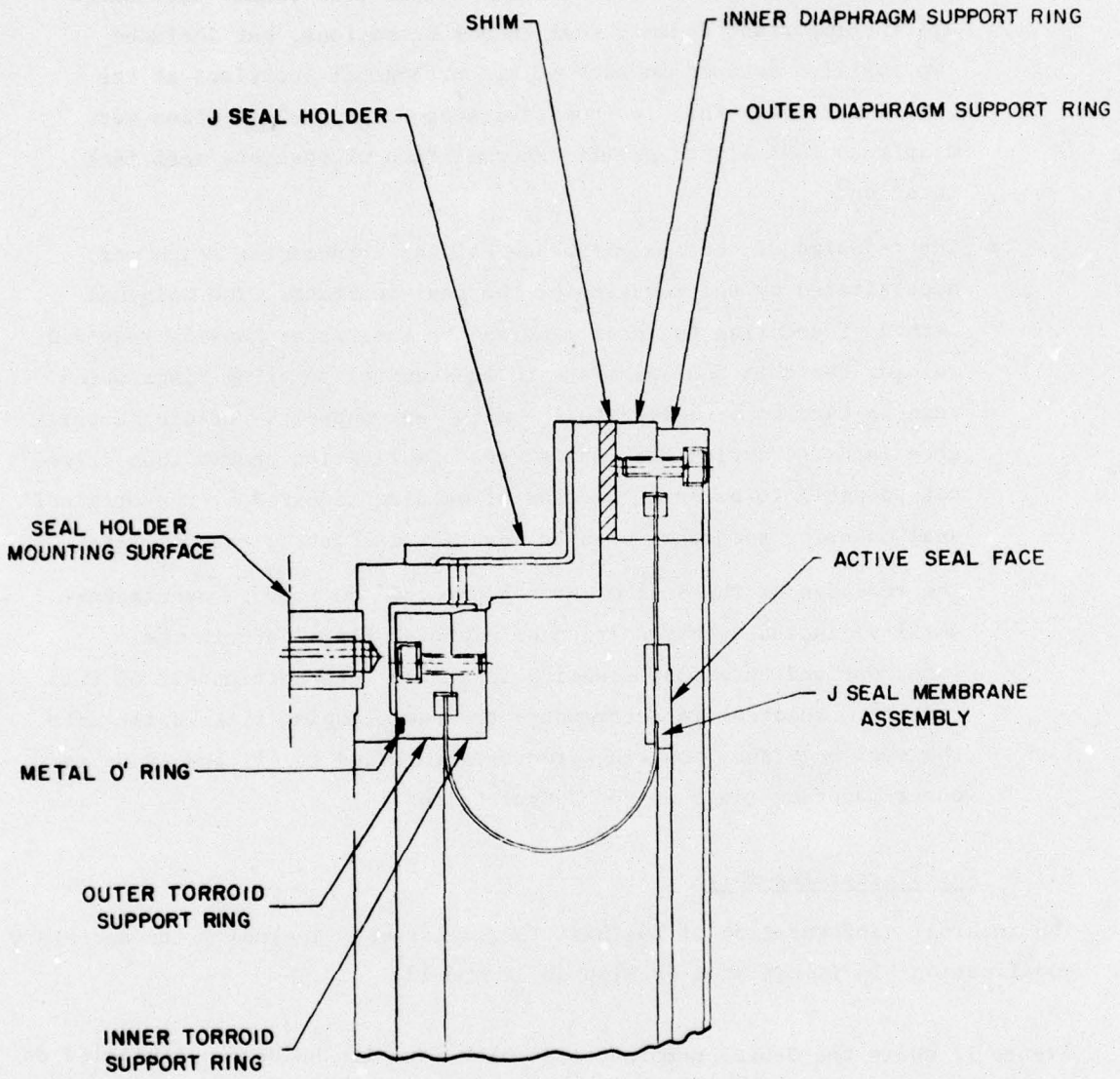

Fig. 11 "J" Seal Assembly

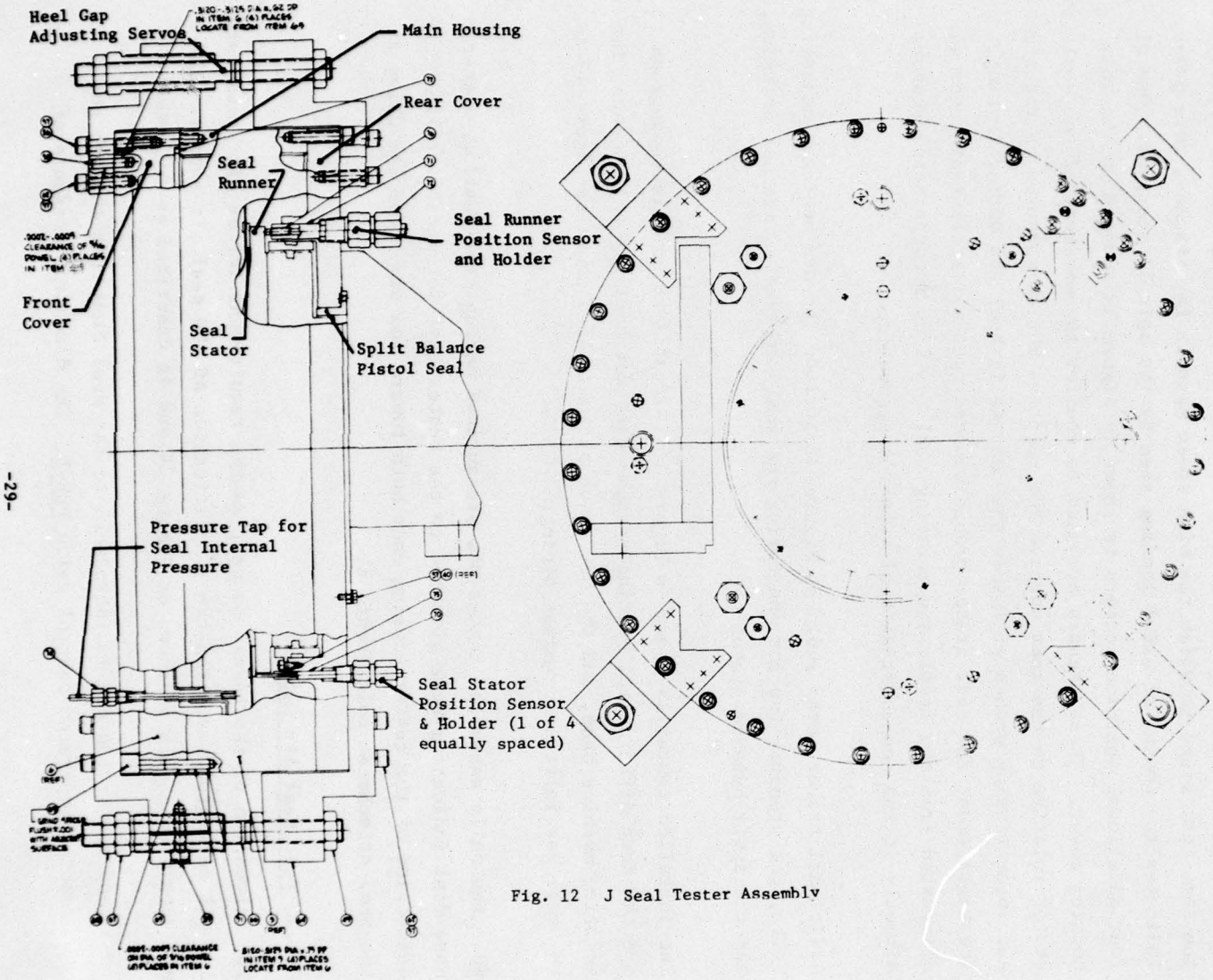

Fig. 12 J Seal Tester Assembly

drawing the tester is shown in the configuration necessary for dynamic, rotational testing. This drawing shows the seal tester, main housing and both the front and rear covers. It is on the front cover that the seal housing (Figure 11) is bolted. Also illustrated on Figure 12 is the location of the position sensor which monitors the relative position of the seal runner relative to rear housing cover. Since this cover is bolted directly on the same test stand to which the high speed spindle is attached, this probe indicates the amount of axial loading seen by the spindle bearings. One of four additional position sensors is shown in Figure 12 mounted in the rear housing cover. These sensors are used to monitor the movement of the seal stator relative to the rear cover. The relative motion measured by the stator and rotor viewing probes will show the changes in heel gap during testing. The requirement for seal stator probes mounted in the testers rear cover was eliminated from the static non-rotating seal tests by incorporating sensors directly in the non-rotating seal runner's active face.

Additional tester parts shown on Figure 12 include the new heel-gap adjusting bolts, the pressure tap for monitoring the seal membrane's internal pressure, and the split balance piston seal.

The installed tester is shown in Figure 13. Identified on this photograph are the four differential bolting systems used for heel-gap adjustments, the modified machine base, and the new drive system. Also shown on Figure 13 is the seal gas inlet and exhaust piping.

When the fully assembled tester was pressurized during seal testing, magnetic base dial indicators were attached to the tester base for measuring the deflection of the tester housing ends both toward and away from the drive at the seal attachment bolt location.

6.1.3 Test Seal Air Supply

The relocation of the tester as well as the requirement for an air accumulator and oil separator permitted the simplification of the seal air supply. The air supply schematic is shown on Figure 14 and is described as follows.

> Shop air at 100 psi is introduced to the seal flow loop through the remotely operated control valve PCV-1. The discharge pressure of

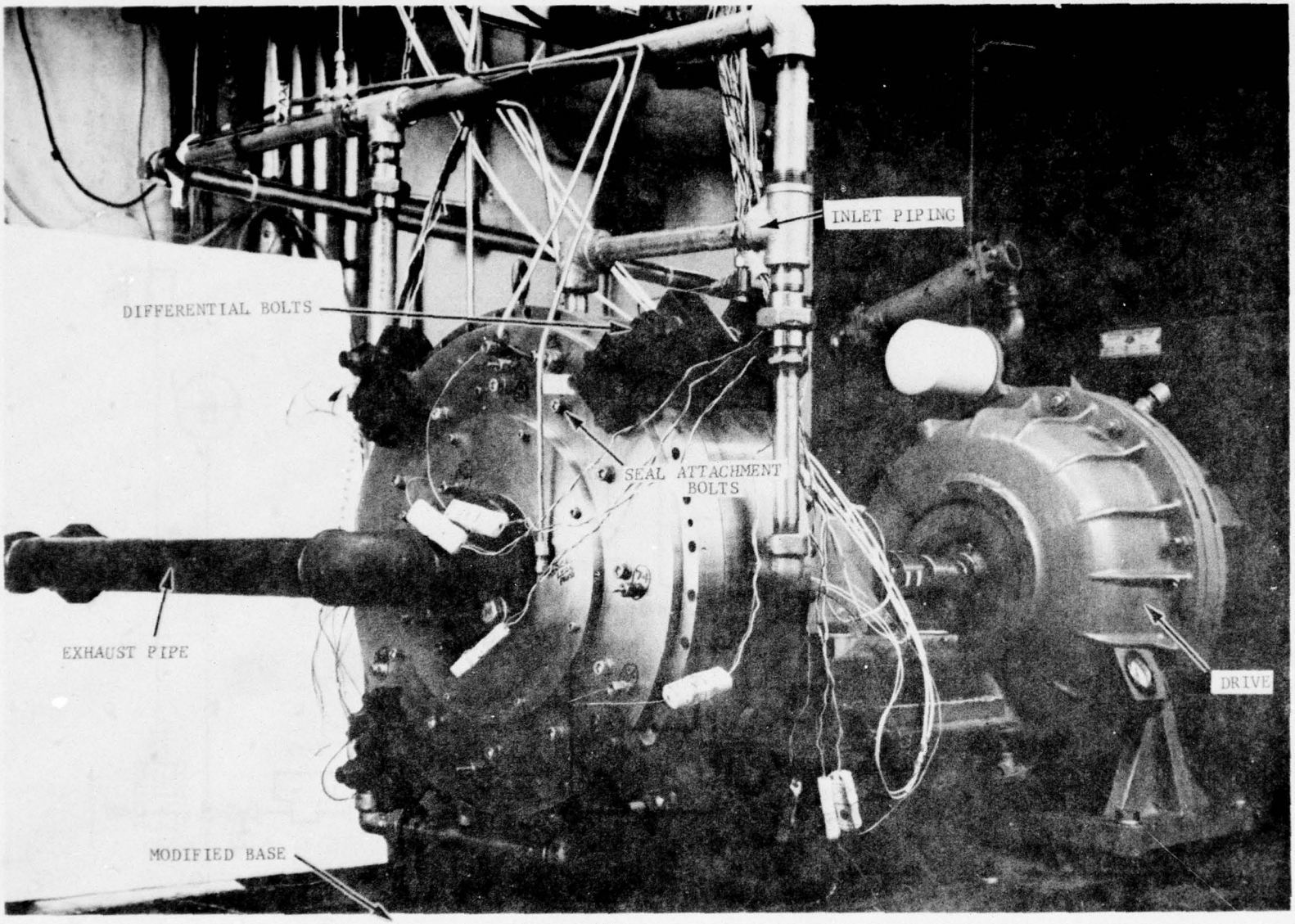
INLET PIPING
DIFFERENTIAL BOLTS
SEAL ATTACHMENT BOLTS
EXHAUST PIPE
DRIVE
MODIFIED BASE

Figure 13

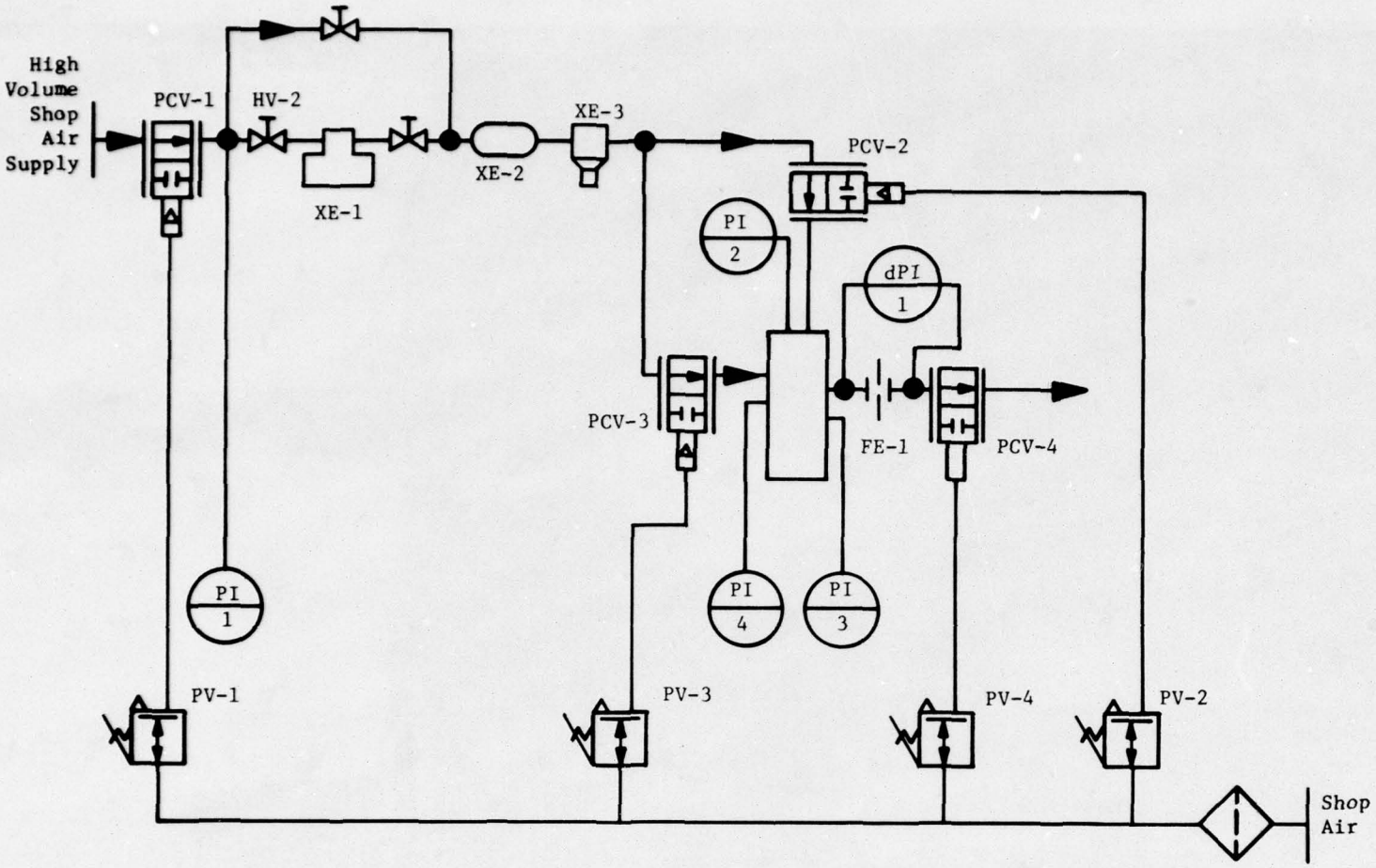

Fig. 14 Seal Air Supply Schematic

this valve is read out in the control room on the pressure gage PI-1. At this point the flow of air can be directed to the high pressure piston compressor XE-1, through the accumulator XE-2, and to the combination oil separator trap XE-3. By closing the by-pass valve HV-1 and opening the two through valves, HV-2 and HV-3. If low pressure air is required, valves HV-2 and HV-3 can be closed and HV-1 opened to allow air to flow through the by-pass loop around the piston-compressor.

Air exiting the separator flows through a remotely operated seal pressure control valve, PCV-2 into the seal inlet port, a pressure gage PI-2 is used to measure the seal inlet pressure. A secondary air supply obtained from the separator discharge line is directed through the balance piston pressure control valve PCV-3 into the balance piston. The balance piston pressure is measured by the pressure gage PI-4.

After the pressurized air passes through the test seal and enters the seal discharge piping, it passes through an orifice plate flow meter FE-1 and through a back pressure control valve PCV-4. The pressure drop across the orifice flow meter is measured by the differential pressure gage dPI-1; the seal discharge pressure (the orifice flow meter inlet pressure) is measured by the pressure gage PI-3.

During seal testing PCV-1 is set to maintain a constant inlet pressure to the flow loop regardless of the demands from other plant facilities connected to the same supply. PCV-2 is then adjusted in conjunction with PCV-4 to establish the desired seal inlet pressure and seal pressure drop. As PCV-2 and PCV-4 are incrementally adjusted, PCV-3 is used to maintain proper balance piston performance.

Control air for all the remotely operated valves is supplied by a separate shop air connection. The control air is filtered prior to use and is used to operate the control valve by adjustment of the pressure regulators PV-1 through PV-4.

6.2 Instrumentation

Instrumentation was incorporated in the J-Seal Tester Assembly to monitor

and measure the following quantities:

- Gap between static seal runner and seal stator
- Position of seal runner relative to tester housing
- Position of seal stator relative to housing
- Temperature of seal stator
- Temperature of seal static runner (at position sensor locations)
- Temperature of seal housing
- Pressure at seal inlet
- Pressure at seal discharge
- Pressure at balance piston
- Strain of seal membrane

The location of the position and temperature sensors relative to the test seal is indicated on Figure 15. Position sensors B_1 and B_2 are firmly mounted into the static seal runner at one radial location, but are displaced radially to permit measurement of possible seal stator rotation as well as any translation. A similar pair of sensors, B_3 and B_4 are displaced circumferentially 90^o from the B_1, B_2 sensors to assist in determining the existance of non-symmetrical seal motion.

Two thermocouples, TC_1& TC_2, each provide a measurement of the non-rotating seal runner temperature at the two probe pair locations.

The position of the seal-gap sensors on the non-rotating seal runner is illustrated by the photograph on Figure 16. At each probe location, a counter bore and lead wire slot were machined into the seal face. Into each counter bore a special eddy current proximity probe was glued with a high-temperature epoxy. The epoxy was then machined to conform with the contour of the seal's active surface. Coaxial lead wires from all four probes were bundled together and led out of the tester through a pressure-tight connector.

A fifth position sensor, B-5, mounted on the tester housing measures the movement of the seal runner relative to the tester housing.

A sixth position sensor, to be employed during rotational tests when the static seal runner cannot be used, is to be mounted in the tester's front cover. This

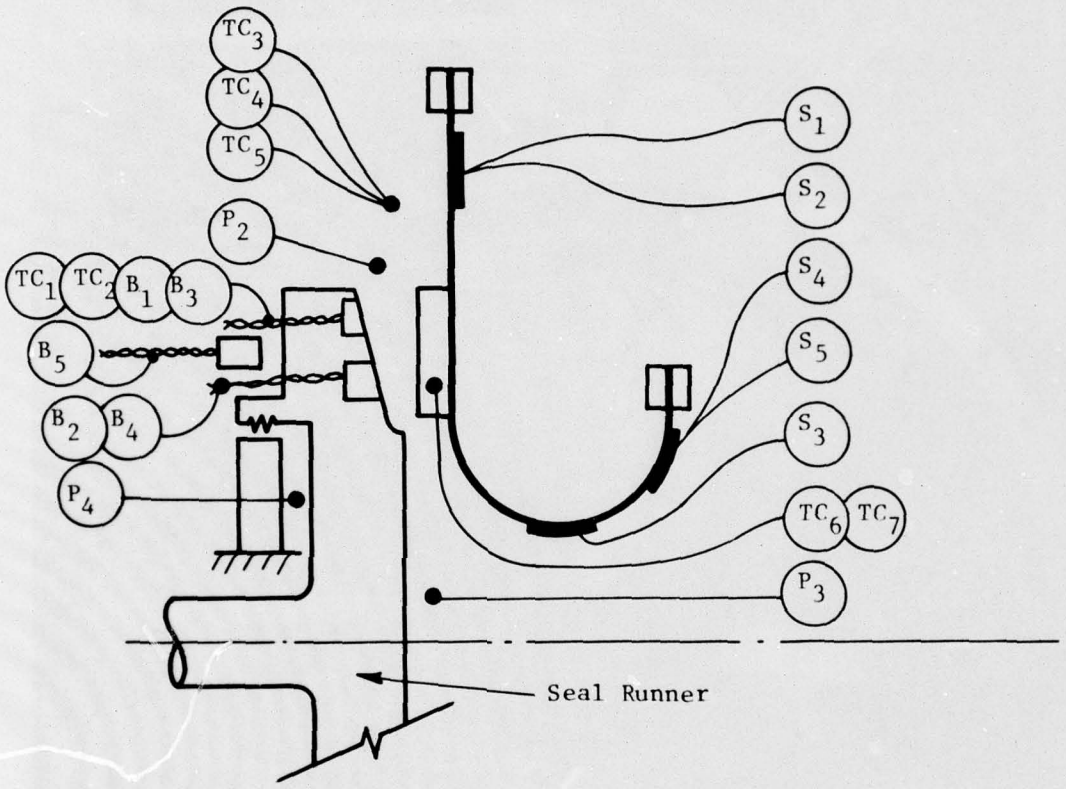

Fig. 15 Instrumentation Locations - Static Seal Test

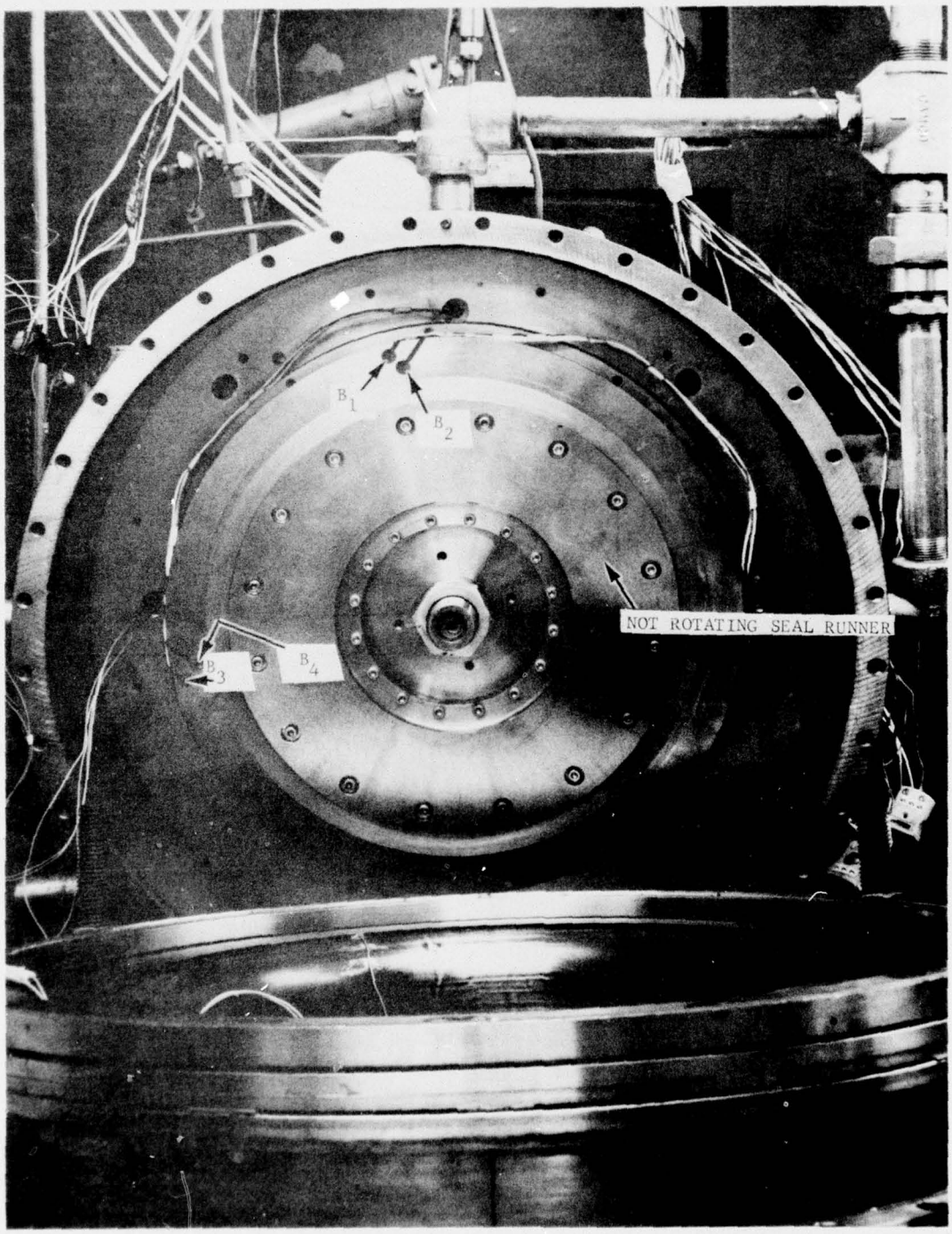

Fig. 16 Position Sensor Location on Non-Rotating Seal Runner

probe will measure the movement of the test seal relative to the tester housing at a radius just beyond the radial extent of the seal runner.

The reading of these sensors is used to judge the level of pressure required in the balance piston at P_4 to counter the seal pressure loading on the test spindle bearings.

Two additional pressure readouts are provided at P_2 & P_3 to establish the operating pressures at the seal inlet and at its exhaust. Thermocouples TC_3, TC_4, and TC_5 are provided to measure the seal inlet gas temperature.

The measurement of seal strain and static seal runner temperature are taken with five strain gages S_1 through S_5 and the thermocouples TC_6 and TC_7. The location of the instrumentation is identified on the photograph of the instrumented test seal, Figure 17.

6.3 Assembly Procedure

In view of the fine dimensional finishes required for a meaningful seal evaluation, particular attention had to be paid to the assembly of the seal component and its installation in the test rig. Following is a description of the assembly procedures developed in the course of this program.

6.3.1 Assembly of Seal Component

After the successful brazing operation described in Section 5.3 was accomplished, the face of the brazed seal component had to be finish machined to establish the required flatness. Since no experience on practical flatness tolerances was available for flexible face type seals, the permissible limits were arbitrarily fixed by limiting the distortion to a value smaller than the minimum operating heel gap which in this case was equal to 0.001 inches.

The analysis discussed in Section 4.0 indicated that the tolerance of the seal to changes in taper is fairly high because the leakage undergoes only very small changes as a function of change in film taper. On this basis the required tolerances on the finished taper were limited to a variation of $\pm$0.002 inches from an established base line.

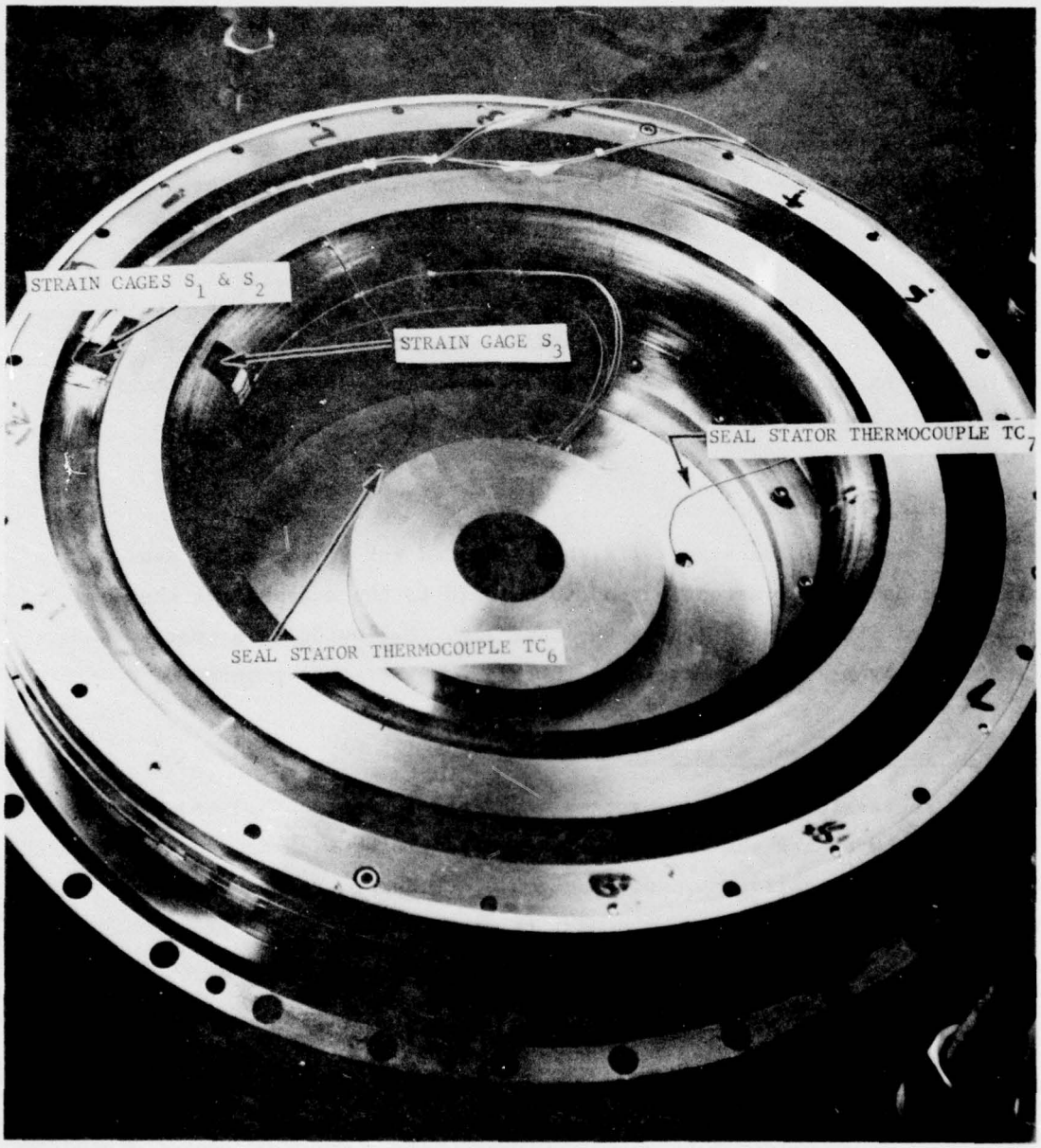

Fig. 17 Instrumentation Location: Test Seal

To machine the seal faces the toroidal portion of the seal was filled with Rigid-ex and its face ground flat. After the machining operation the faces were checked for flatness and were found to be consistently flat within 0.001 inches. The removal of the Rigid-ex, however, resulted in an apparent distortion of the seal face which brought it out of tolerance. Subsequent clamping of the seal in its support housing also appeared to change the distortion pattern.

In order to bring back the seal face within the specified tolerance range, shims were introduced under each cross-bolt at the seal outer end. Careful selection of the shim thickness resulted in the flatness shown in Figure 18. Note that the flatness at the heel gap (where the film thickness is at its minimum) varies only by ± 0.00075 inches. Photographs of the active and passive sides of a fully assembled seal showing the place where the shims were introduced are presented in Figures 19 and 20.

6.3.2 Installation of Seal in Test Rig

When the seal face was found to be in a satisfactory condition, the seal was mounted in the test vehicle and the unloaded heel gap was set with the use of the differential bolting arrangement shown in Figure 13. The heel gap dimensions were read on Probes B_2 and B_4. To maintain the unloaded heel gap setting uniform over the full seal face circumference the rotor was rotated by hand over 180 degrees and readings taken. The adjustments required to bring about a uniform heel gap reading about the circumference were performed through the use of the individual differential screws.

Once satisfactory heel settings were obtained, the differential screws were affixed in place through the locking nut arrangement provided for this purpose and the seal housing pressurized to check for casing leaks. It was during the pressurization process that deflections of the front and rear end of the casing were noted. These deflections result in an effective movement between the seal reference base and the runner, thus upsetting the initially set unloaded heel gap. To correct for the casing deflections two dial gages were mounted, one in the front and the other one in the rear of the casing, and readings of casing deflections were taken at each test point. These readings, together

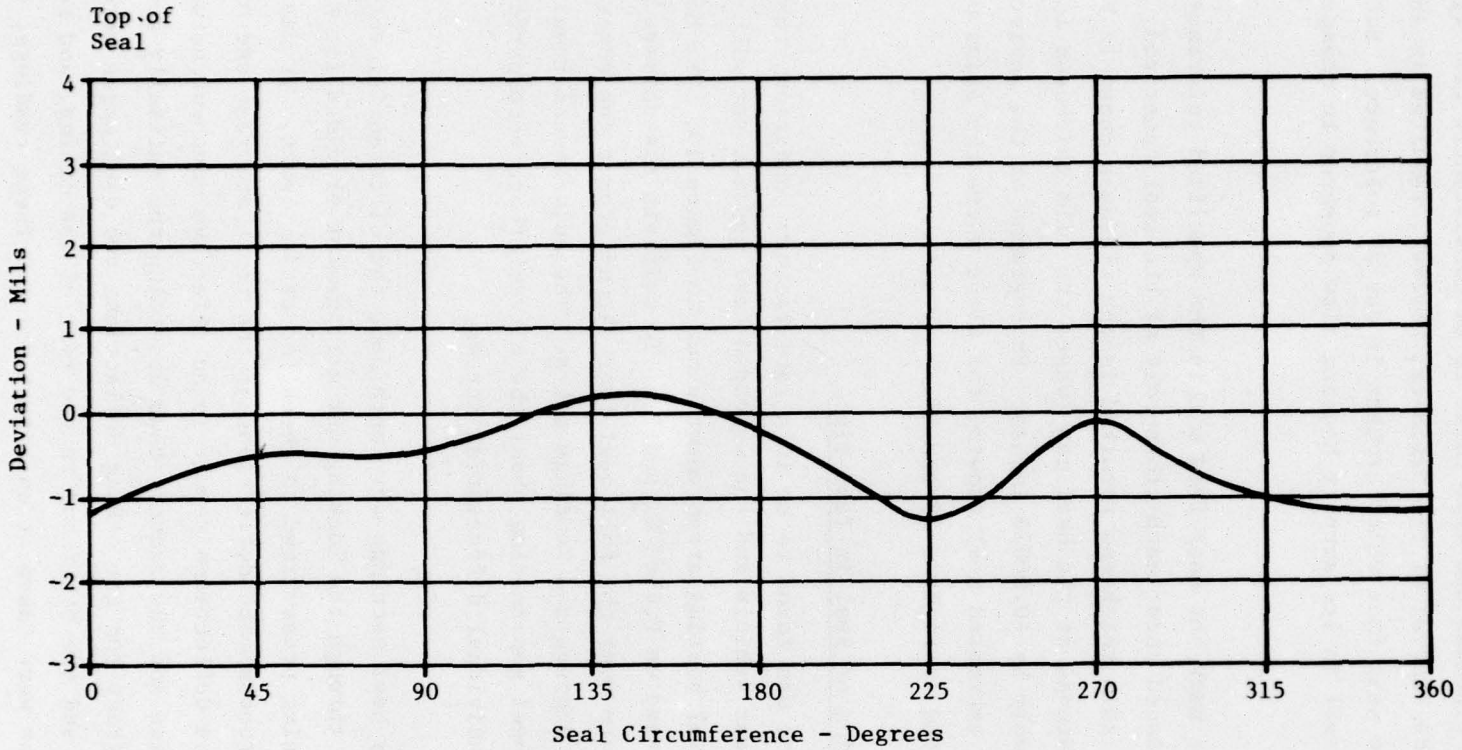

Fig. 18 Seal Face Distortion at Heel Gap

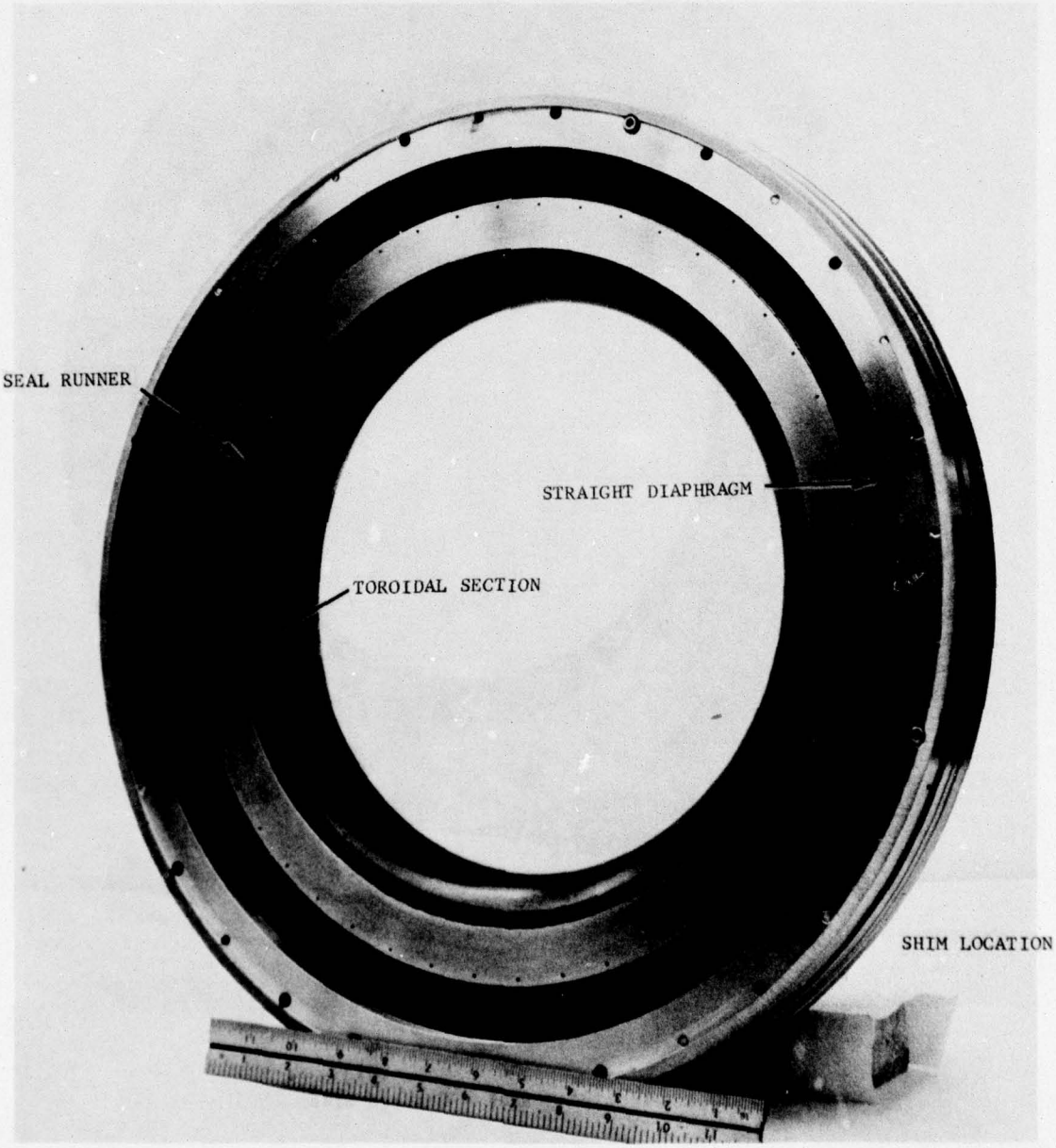

Fig. 19 Assembled J Seal – Active Side

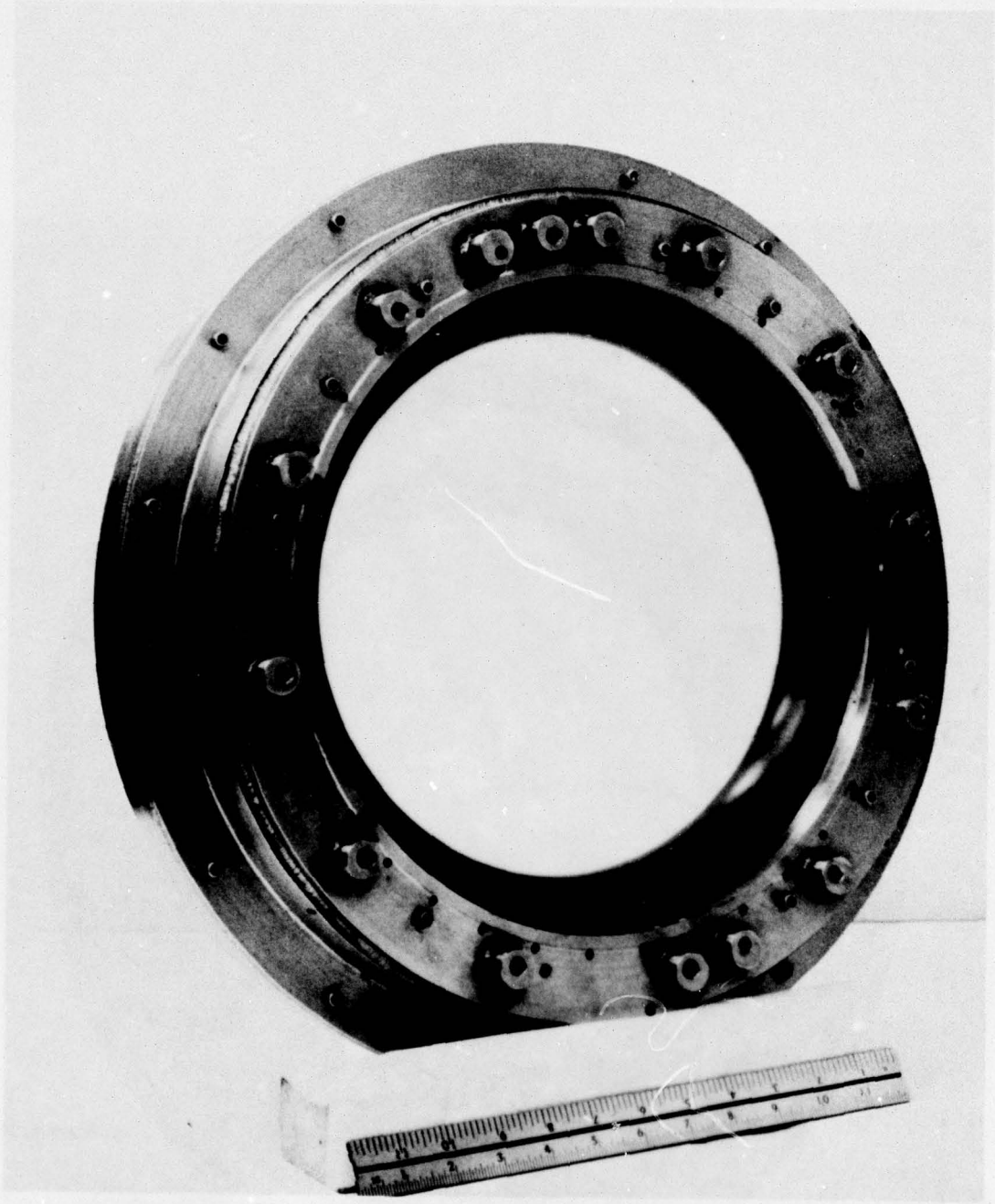

Fig. 20 Assembled J Seal - Passive Side

with the readings of Probe B_5 were then used to establish the corrected unloaded heel gap setting. Details of the correction procedure are described in Appendix A. Once the proper unloaded heel gap setting was obtained and the housing deflection indicators were zeroed out, the unit was ready for test.

6.4 Test Procedure

The procedure worked out for the following sequence of tests consisted of:

1. Mounting of the assembled test seal in the test fixture.
2. Setting of the unloaded heel gap.
3. Taking of initial set of zero pressure readings.
4. Recording of the seal data under pressure.
5. A recheck of the initial readings at zero pressure.
6. Correction of proximity probe readings for:
   - temperature effects
   - proximeter probe spacing
   - differential seal motion due to pressure.
7. Calculation of seal leakage flow.

The data to be recorded consisted of a set of pressure, temperature, proximeter, and strain gage readings. The calibration probes employed to correct the readings for the effects mentioned above are given in Appendix A. A typical data sheet and an explanation of the pressure, temperatures, proximeter, and strain gage readings taken for each test point is given in Appendix B.

SECTION VII
DISCUSSION OF TEST RESULTS

Because of the brazing problems described in Section 5.3, the testing was limited to the seal with a membrane of 0.025 inches thickness.* The 0.020 inch thick sample was badly damaged during the brazing operation and the 0.035 inch sample exhibited distortions and would require additional lapping in the assembled condition before final assembly for test.

The seal runner drawings contained a taper falling within the 0.0055 to 0.0079 inch tolerance range yielding a nominal value of 6.7 mils per inch. The Δh_o under normal conditions should thus have been about 5 mils. The measured Δh_o in the assembled condition fell between 6 and 7.2 mils. This difference is mainly due to the fact that the stationary seal face exhibited a taper on its own (see Section 6.4.1).

Although a 300 psi source was available within the system, the actual test pressures did not exceed 100 psi because, as will be shown later, of the intrinsic behavior of the complete seal. A table summarizing all the test data obtained is given in Appendix B.

The test commenced with an unloaded heel gap setting of 1.1 mils. At first the readings on all instruments were recorded in the as-assembled condition with no pressure applied. The test data is shown in Table 5. Note that the data recorded for Test No. 1 consists only of the initial heel gap and taper settings. In test No. 2 the pressure differential of 37 psi was applied to the seal. This pressure was subsequently raised to 80.5 psi in Test No. 3. Test No. 4 was run without pressure in order to observe whether any permanent changes in the original setting have taken place. The same procedure was repeated for the data shown in Table 6 with an initial heel gap setting of 0.003 inches rather than the 0.001 inch used in the series of tests recorded in Table 5. Table 7 presents the data for an unloaded heel gap setting of 4.5 mils, and Table 8 the data for an unloaded heel gap setting of 7.5 mils.

The data given in all the tables have been corrected for the effects of temperature, differential seal motion, and probe spacing. A detailed discussion of the correction factors is given in Appendix A.

*The minimum thickness on the toroidal section

TABLE 5

TEST RESULTS WITH AN UNLOADED HEEL GAP SETTING OF $\simeq$ 0.001 INCH

Test No.	h_o* Mils	h_∞ Mils	Δh_o Mils	Δh_∞ Mils	Q SCFM	ΔP PSI	P_2 PSIG
1	1.1	-	6.1	-	-	-	-
2	1.8	0.8	-	5.6	32.1	36.6	37.0
3	2.3	0.4	-	6.0	77.1	79.0	80.5
4	0.9	-	6.5	-	-	-	-

*Variation in unloaded heel gap is due to effects of case pressure on original unloaded heel setting.

TABLE 6

TEST RESULTS WITH AN UNLOADED HEEL GAP SETTING OF $\simeq$ 0.003 INCH

Test No.	h_o Mils	h_∞ Mils	Δh_o Mils	Δh_∞ Mils	Q SCFM	ΔP PSI	P_2 PSIG
5	2.8	-	7.2	-	-	-	-
6	3.5	1.0	-	7.0	41.3	35.5	35.0
7	4.0	0.7	-	7.0	86.3	78.0	80.0
8	2.7	-	7.2	-	-	-	-

TABLE 7

TEST RESULTS WITH AN UNLOADED HEEL GAP SETTING OF $\simeq$ 4.5 MILS

Test No.	h_o Mils	h_∞ Mils	Δh_o Mils	Δh_∞ Mils	Q SCFM	ΔP PSI	P_2 PSIG
9	4.4	-	6.6	-	-	-	-
10	Seal blows open when 35 psi is applied.						
11	7.6	7.6	-	3.5	10.5	12.0	15.0
12	11.7	13.3	-	6.1	25.9	5.5	20.0
	Seal suddenly begins to open at P_2 = 15 psi and remains open when pressure is increased.						

TABLE 8

TEST RESULTS WITH AN UNLOADED HEEL GAP SETTING OF $\simeq$ 7.5 MILS

Test No.	h_o Mils	h_∞ Mils	Δh_o Mils	Δh_∞ Mils	Q SCFM	ΔP PSI	P_2 PSIG
13	7.56	-	6.0	-	-	-	-
14	-	6.9	-	5.2	12.21	8.5	12.5
	Seal begins to open when P_2 = 12.5 psi is exceeded.						

Because the original analysis was performed for pressure differentials of 250 and 500 psi, and the actual tests were run on air pressure below 100 psi, the comparison between the test data and analytical results can at best be qualitative rather than quantitative. Tables 9 and 10 present a comparison of the general trends registered on the pertinent seal performance parameters on test and analyses. The analytical results were obtained from Figures 21 and 22.

TABLE 9

COMPARISON OF TEST AND ANALYSIS

(CONSTANT PRESSURE)

	Test Data - $\Delta P \simeq 80$ PSI					Analytical Data - $\Delta P \simeq 250$ PSI				
Test No.	h_o mils	h_∞ mils	Δh_o mils	Δh_∞ mils	Q SCFM	h_o mils	h_∞ mils	Δh_o mils	Δh_∞ mils	Q SCFM
3	2.3	0.4	6.1	6.0	77.1	10	1.2	6.4	9.3	122
7	4.0	0.7	7.2	7.0	86.3	15	2.6	6.4	10.0	325

TABLE 10

COMPARISON OF TEST AND ANALYSIS

(CONSTANT HEEL GAP SETTING)

	Test Data - $h_o \simeq 3$ mils					Analytical Data - $h_o \simeq 10$ mils				
Test No.	h_∞ mils	Δh_o mils	Δh_∞ mils	ΔP psi	Q SCFM	h_∞ mils	Δh_o mils	Δh_∞ mils	ΔP psi	Q SCFM
6	1.0	7.2	7.0	35.5	41.3	1.2	6.4	9.3	250	122
7	0.7	7.2	7.0	78.0	86.3	0.8	5.9	8.5	500	203

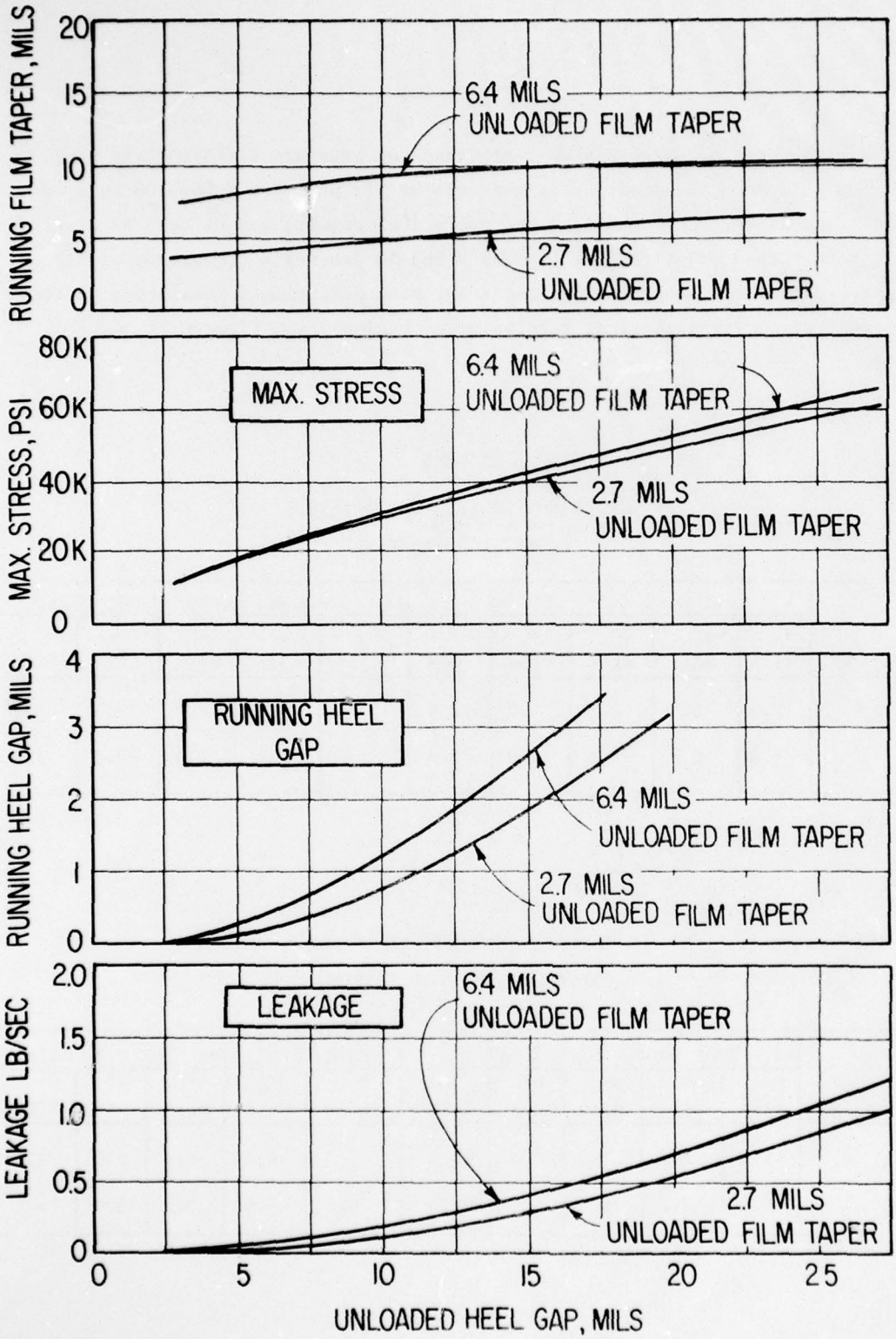

Fig. 21 Performance Curves For Test Model Geometry At Two Values Of Unloaded Taper. ΔP = 500 psi

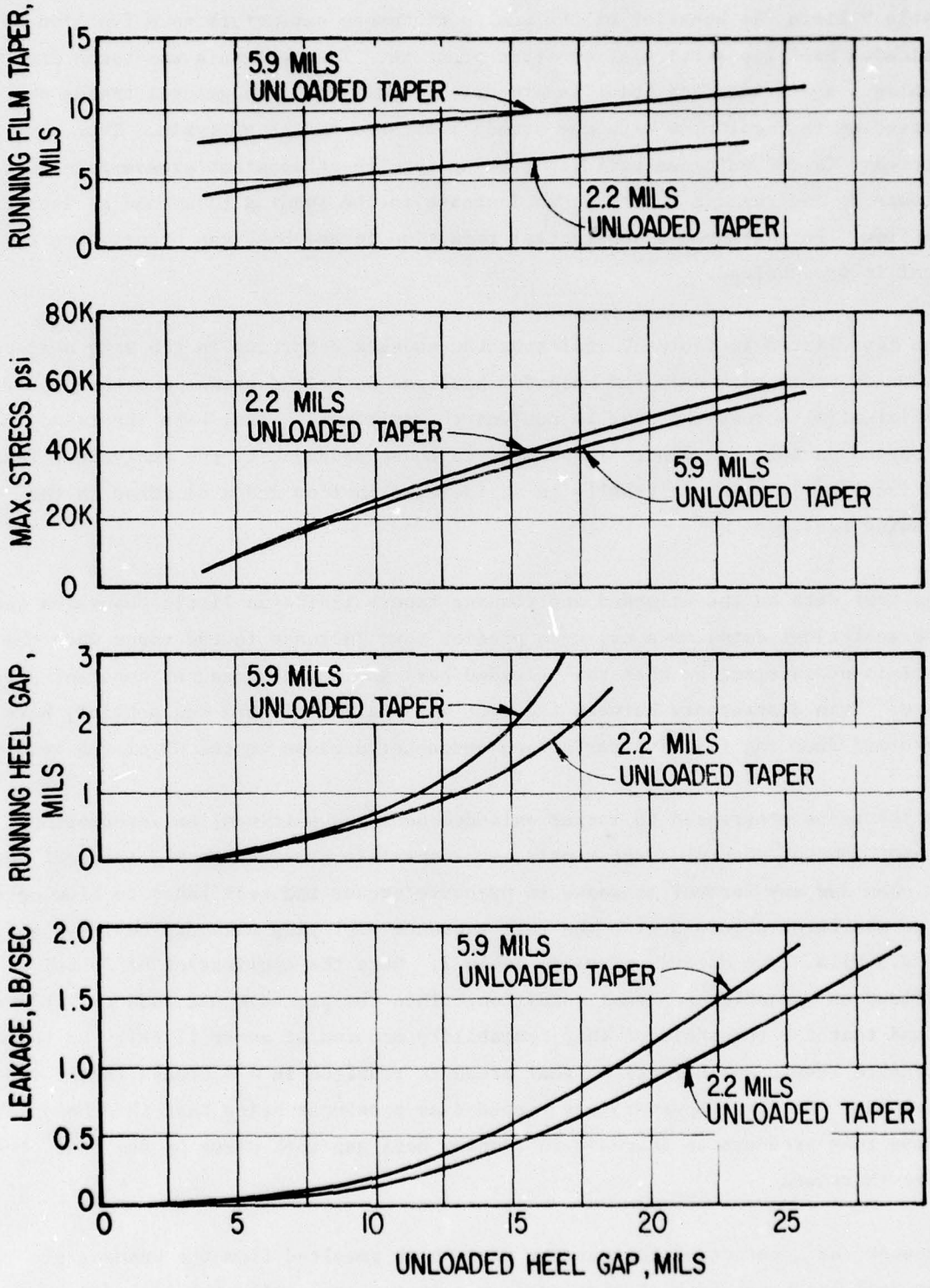

Fig. 22 Performance Curves For Design Geometry At Two Values Of Unloaded Taper. ΔP = 500 psi

Table 9 lists the behavior of the seal performance parameters as a function of unloaded heel gap setting at constant pressure. The test data was taken from Tables 5 and 6 and each point is properly identified. The general trends observed on test coincide with the trends indicated by the analysis. Thus, an increase in the unloaded heel gap setting results at constant pressure in an increase in the running heel gap, an increase in the running taper and an increase in flow. Furthermore, a substantial reduction in the heel gap occurs when the seal is pressurized.

The data listed in Table 10 indicates the changes occurring in the same seal performance parameters when the unloaded heel gap is held constant and the pressure differential across the seal is subject to variation. Also, here the trends observed on test are generally similar to those produced by the analysis. Thus, an increase in pressure results in an increase in flow and a decrease in the running heel gap.

The test data on the unloaded and running tapers indicates little change on test. The analytical data, however, does predict some increase in the taper when the seal is pressurized or when the unloaded heel gap is increased at constant pressure. This discrepancy between the test and analytical data can possibly have resulted from the flatness variations encountered close to the OD of the test seal.

As the tests progressed to larger unloaded heel gap settings, an interesting phenomenon was observed; apparently, at a specific pressure level, the seal begins to open and any further increase in pressure causes the seal faces to blow open. This was first observed with the test sequence employing unloaded heel gap setting of 4.5 mils. The data is given in Table 7. Here the application of 35 psi yielded an unstable open seal condition. Then the pressure was reduced, it was found that the threshold of this instability occured at about 12 psi. Up to that pressure level, an increase in seal pressure resulted in a decrease in the running heel gap. No data, however, was recorded at pressures below that threshold level. Above that pressure an increase in running heel gap took place as the seal pressure increased.

Because the substantial increase in flow which resulted from the opening of the heel gap produced high case pressures at the seal exit, the unloaded heel

gap setting also underwent substantial changes. The increased case pressures resulted in increased casing deflections which had the effect of increasing the unloaded heel gap setting.

The tests were repeated with an unloaded heel gap setting of 7.5 mils. It was noted that in this case also, the seal began to open up at a pressure of about 12.5 psig. Test results are listed in Table 8.

Although this seal instability was at first glance surprising, a closer examination of the data provided by the analysis also indicates the presence of a potential trend in this direction. This can be noted in Figures 21 and 22 which have been reproduced from Reference 1. In Figure 21, and particularly in Figure 22, the running heel gap increases at an extremely fast rate with an increase in the unloaded heel gap setting when the latter exceeds 10 mils. As a matter of fact, Figure 22 indicates that with an unloaded taper of 5.9 mils, the increase in running heel gap almost approaches a vertical asymptote in the vicinity of a heel gap setting of about 17 mils. Thus, at least qualitatively speaking, the seal blow-up phenomenon is also predicted by the analysis, but the pressure levels at which the blow-up occurs are considerably different.

Although it is apparent that this type of instability is highly undesirable in any practical face type seal application, it is equally apparent that with proper design precautions such instabilities can be avoided. In an actual application the concept of an unloaded heel gap setting will not exist. This concept was literally invented to render the initial testing more economical. The "unloaded heel gap" will, in fact, disappear since the axial spring load will always provide sufficient preload to maintain close contact between the stationary seal face and its runner at unloaded conditions, hence the unloaded heel gap will always be zero. This should be clear from an examination of the realistic seal concept shown in Figure 1. It must be recognized, however, that although the unloaded heel gap does not exist in an actual face seal application, the seal can still blow open if improperly designed. This is true for all face type seals. The possibility of the seal blowing open can be eliminated by proper seal balance where the balance of forces acting on the seal face is such that the force generated at the seal interface cannot overcome the seal closing forces.

In summary, the results of the test disclosed good qualitative agreement between the analysis and test. The seal instability encountered at higher pressure, however, prevented seal runs at elevated pressure levels. The limitations imposed by these instabilities can be eliminated by the use of a realistic seal configuration in future tests. The results obtained on these tests also indicated that any future work on this sealing concept should also address itself to the quantitative aspects of analytical verification and attempt to explain the apparent discrepancies between the analysis and test pressure levels at which the seal instability occurred.

SECTION VIII

CONCLUSIONS

The test data cited in this report is in good qualitative agreement with the analytical predictions. The increase in running heel gap with an increase in the unloaded heel gap, the decrease in running heel gap with increase in pressure, and the increase in leakage flow with increase in unloaded heel gap setting and increase in pressure predicted by the analysis was also recorded on test.

The tested seal geometry disclosed the presence of a "run-away" condition at which the seal blows open at a certain pressure level and any subsequent increase in pressure will widen the running heel gap and result in increased flow. This condition arises only at or above a certain heel gap setting, and can be avoided by maintaining originally low heel gaps. Although the above described behavior was not originally noticed in the analytical calculations performed in Phase I, a re-examination of the data does indicate a threshold for the unloaded heel gap setting beyond which the "run-away" condition may develop.

The seal configuration which was subjected to test is representative of a simplified seal arrangement. In this arrangement the unloaded heel gap setting controlled the running heel gap. In a realistic jet engine seal the unloaded heel gap setting will be always zero (contact between runner and stator will always be present at static conditions) hence, the "run-away" condition described above is less likely to occur.

Finally, within the scope of this program, an acceptable functional brazed joint capable of operation at high temperature was developed and one sound and accurate seal was produced for test purposes. Out of the total of three seal samples originally planned, one was destroyed in the brazing process and one was deemed not sufficiently accurate dimensionally to warrant further testing.

SECTION IX

RECOMMENDATIONS

The feasibility of the "J" seal concept and the qualitative value of the seal analysis (Reference MTI Report MTI-75TR59) has been tentatively established as a result of the test program presented in this report. It is recommended, however that no further testing of the presently constituted J-seal model be performed.

The reasons for not pursuing the testing of the present "J" seal model are described as follows:

- The present test seal configuration is not representative of a realistic engine seal since it contains no secondary seal carrier. The lack of the secondary carrier forced the J-seal to be tested at fixed, preset heel gap settings which resulted in seal blow-out at very low pressure differentials.
- Sealing face distortions which were recorded for the test seal, although significantly improved over previous "J" seal models, did not present the type of distortion free surface normally associated with face seals.

A major result of the demonstrated basic "J" seal concept feasibility was the uncovering of a number of problems that need to be overcome. It is recommended therefore, that further development work be directed toward the following tasks, and preferably also in that order.

9.1 Incorporation of Secondary Seal

It is apparent that for the "J" seals, to perform properly, it must be mounted on a secondary seal carrier, therefore it is proposed that a revised seal design be prepared which incorporates an appropriate secondary seal carrier. In addition, improvements to factors such as the diaphragm mounting should be incorporated in any new design. A sketch of a "J" seal with an axially spring loaded secondary seal carrier is shown in Figure 1.

9.2 Modification of Seal Analysis

The seal analysis should be extended to incorporate the operation of the secondary seal carrier. Performance calculations using the analysis should be

made at pressures ranging from as low as 50 psi to 600 psi so that comparison of experiment with theory can be made over the full pressure range.

9.3 Manufacturing Technique

An in-depth study of manufacturing techniques for the preparation of "J" seals should be performed. Special emphasis should be placed on the attainment and retention of dimensional accuracy. The advancements in the brazing technique reported herein can be used as a cornerstone for this study.

9.4 Room Temperature Seal Test

It is recommended that a full scale model based on the results of 9.1 be manufactured and tested at room temperature conditions with pressures up to 300 psi and speeds up to 12,000 rpm. The seal test rig should be further modified to permit measurement of primary seal profile and film thickness during operation at speed. The value of having film thickness data on the active face has been demonstrated, and with the current instrumentation this information cannot be obtained during rotational testing. It is recommended that film thickness instrumentation be mounted on the runner similar to the type which has been developed and demonstrated on a high speed foil bearing test program for NASA.

9.5 High Temperature Seal Test

Following the resolution of any dynamic or operational problems arising from the tests in 9.4 above, a seal capable of operating at full pressure up to the maximum desired operating temperature should be fabricated and tested under simulated jet engine conditions.

In summary the test data obtained to date indicate trends in performance which require further study. The ability of a "J" type seal to function in an actual engine environment requiring both high temperature and high pressure performance capability as indicated by the test matrix specified in the present contract will eventually have to be demonstrated on test. However, the difficulties encountered in testing the present seal without a carrier, as enumerated previously, indicate a more cautious step-by-step approach in evaluation is required.

In future work, the basic emphasis of the current test matrix should be retained but the evaluation of J-seal efficiency can be obtained from a somewhat restructured matrix. The restated matrix should be of such form that each major step in test conditions such as elevated test temperature, higher pressures and speed increments are evaluated independently before being tested in combination.

Appendix A

Conversion Factors and Calibration

A. 1.0 Proximeter Probes

The proximeter probes employed in this test setup require voltage to distance conversion curves, temperature corrections, and extrapolation of proximity probe reading from the installed proximeter to the position of minimum film thickness.

The probes were initially calibrated in the "as installed" position using a target made of the same material as the seal face. The distance of the target to probe was varied though the use of extra accurate gage blocks and the voltage corresponding to each distance was recorded. The voltage vs. distance curves which were obtained in that fashion are shown in Figure A-1. Note that separate curves were generated for each probe employed in the test setup.

Proximeters B_1 and B_2 as well as B_3 and B_4 were used in pairs placed 90^o apart. The proximeters with even subscripts were located close to, but not at, the inner edge. Hence, in order to obtain the measurement of the heel gap, the readings obtained with B_{2-4} proximeters had to be corrected to obtain the minimum film thickness (actual heel gap).

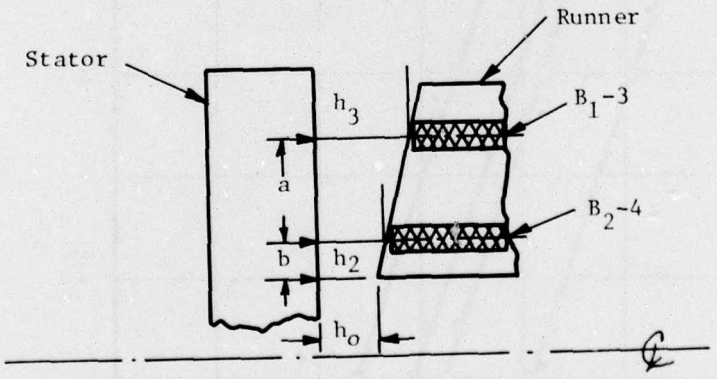

Fig. A-2 Identification of Probe Locations

Referring to Figure A-2 above:

$$h_o = h_3 - \frac{\Delta h_{2-3}}{a}(a + b) \qquad (1)$$

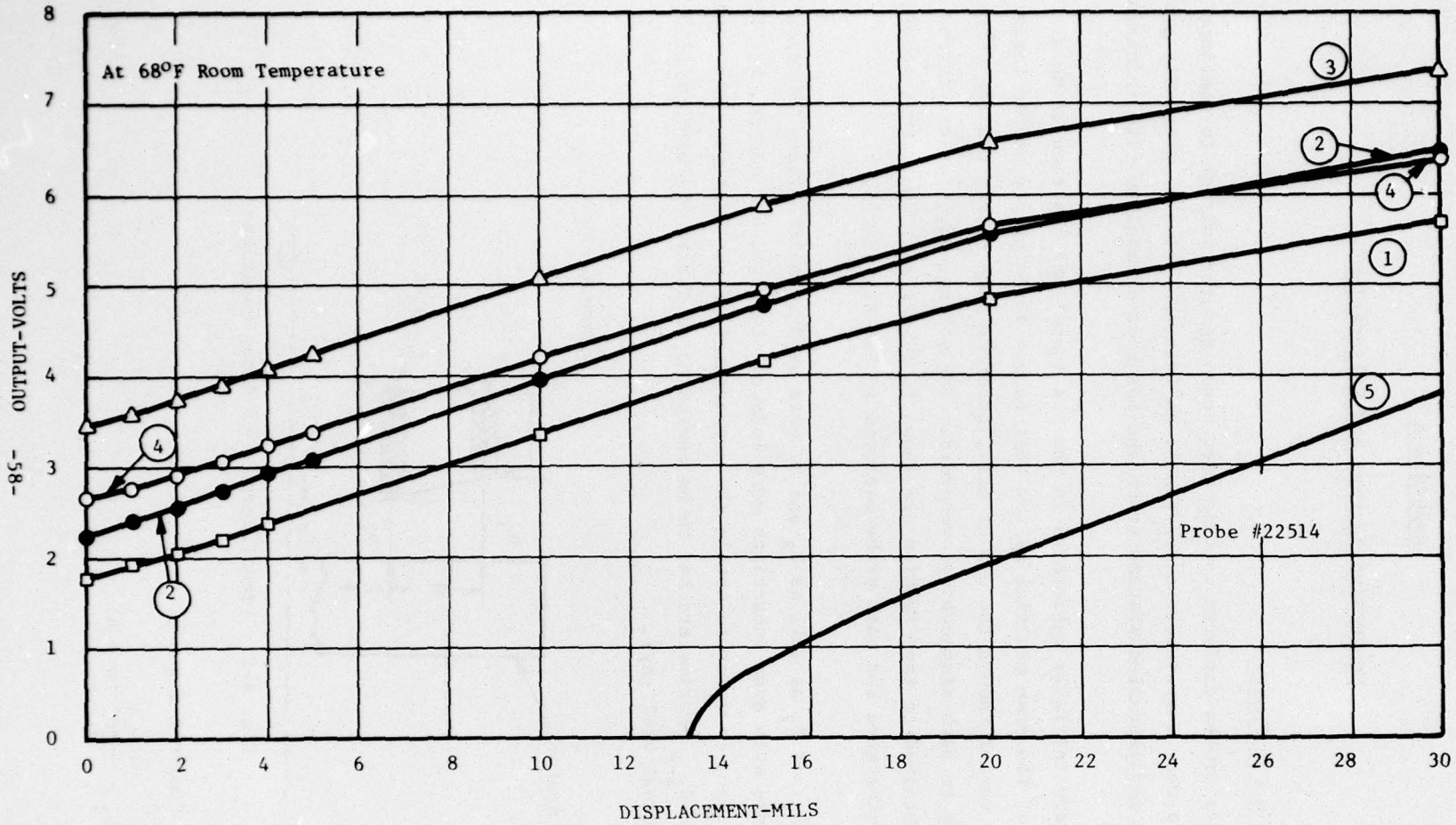

Fig. A-1 Voltage Vs. Distance Curves

Substituting constants

$$h_o = h_3 - 1.22\Delta h_{2-3} \tag{2}$$

The actual $\Delta h'_\infty$ is in a similar way found to be

$$\Delta h'_\infty = \frac{.875}{.37}\,\Delta h_\infty = 2.365\Delta h_\infty \tag{3}$$

In addition to the above corrections it was found that the seal cover and housing moved slightly under pressure. Due to the pressure differential across the runner, the runner position also exhibited a tendency to shift. To establish the extent of movement, dial indicators were applied to the front and rear of casing at the seal bolting circle, and a probe was inserted to measure the relative axial motion between rotor and casing. This motion had the effect of changing the unloaded heel gap setting. To determine the change and correct for it the following relationship was used:

$$\delta_c = \delta_{cf} - (\delta_r - \delta_{cr}) \tag{4}$$

where δ_c is the correction to the unloaded heel gap setting, δ_{cf} the deflection of the front casing, δ_r the relative deflection of the rear casing and runner (B_5), and δ_{cr} the deflection of the rear casing.

Prior to the above correction, the voltage readouts had to be corrected for temperature effects. Because the slopes of the proximeters voltage vs. distance curves were for all practical purposes identical and calibration tests at elevated temperatures have shown that the responses to temperature changes were also very similar, one temperature correction was used for all proximeters; this correction was equal to .014 volts/^oF. Thus, for example, when the temperature of the proximeter on test was 10 F lower than the calibration temperature 0.14 volts was added to the voltage readout and the actual distance determined from Figure A-1. A sample temperature correction curve is given in Figure A-3.

A. 2.0 Flow Calculations

Flow was measured with the use of a square edge orifice plate, a sketch of

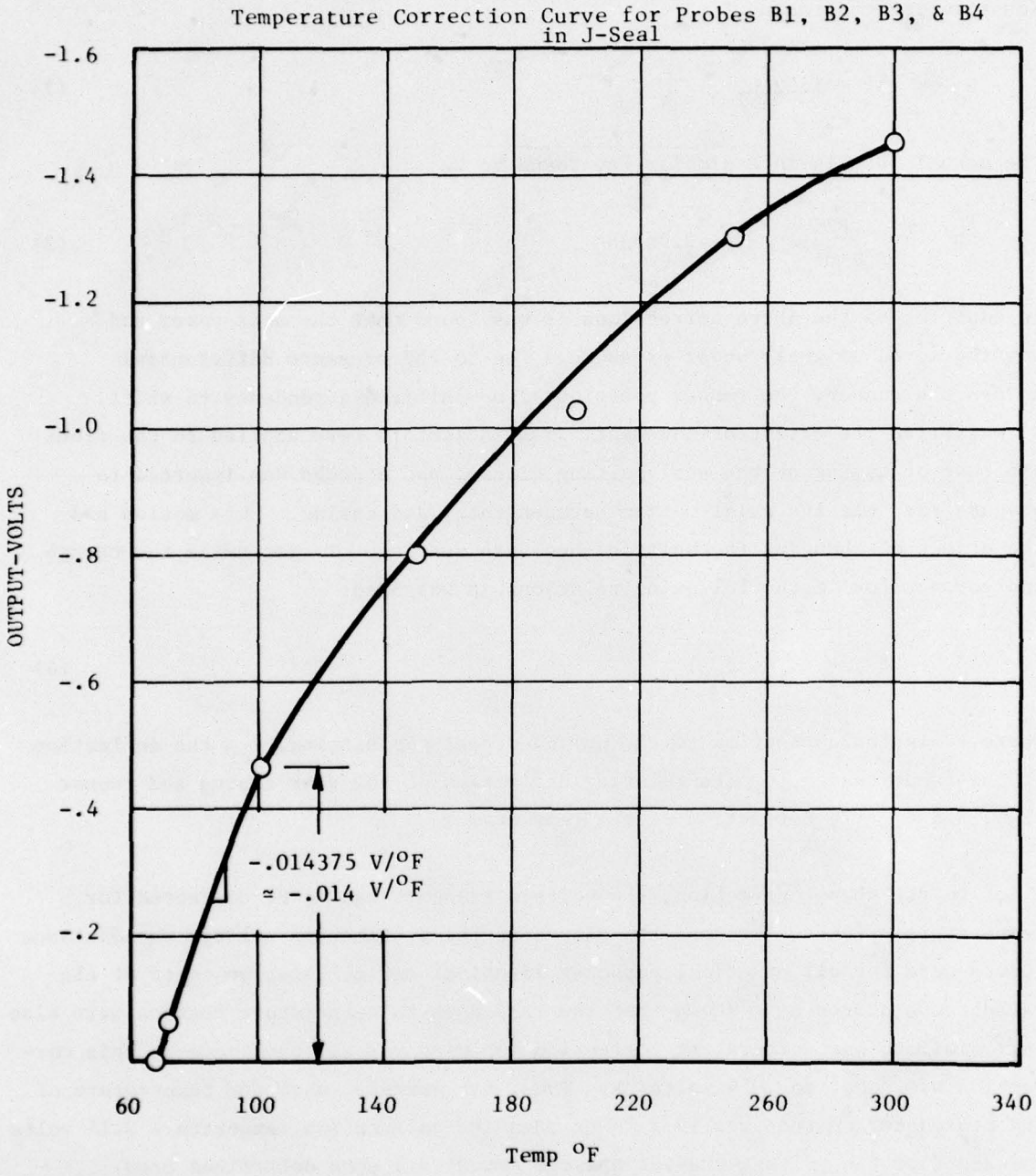

Fig. A-3 Sample Temperature Correction Curve

which is shown in Figure A-4.

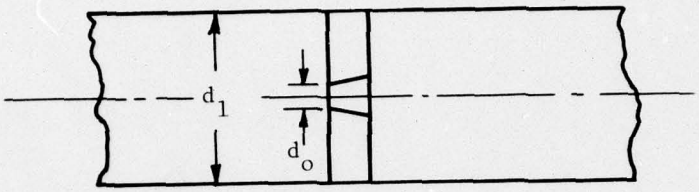

Fig. A-4 Model of Orifice Plate

The equation used was (Ref. 2)

$$Q = YCA\sqrt{29\Delta P\rho}$$

when Y = expansion factor, depends on $\frac{\Delta P}{P_1}$ and ρ, and ∂

C = flow coefficient, depends on $\frac{do}{d_i}$ and R_e (Reynolds Number)

A = area of opening, ft^2

g = 32.17 ft/sec^2

ΔP = pressure difference across orifice (where ΔH is in inches of H_2O)
$5.2\Delta H$

P_c = ft^3/lb_m

r = specific heat ratio

Q = ft^3/sec

R_e is usually very high for air flow (of the order of 10^6), thus, C remained constant at 0.64. The factor Y was found to vary from 0.998 to 0.948, depending on $\frac{\Delta P}{\rho}$. Thus, for all practical purposes the following equation can be used:

$$Q = 2.875 \quad \frac{(\Delta H)T}{P_1}$$

at reference conditions of $P_o = 14.7$, $T_o = 60$ F.

Appendix B

Test Data and Nomenclature

TABLE A.1

STATIC TEST RESULTS WITH ALIGNED SEAL

TEST NO.	P_1 psig	P_2 psig	P_3 psig	P_4 psig	ΔP_1 in. H_2O	TC_1 °F	TC_2 °F	TC_3 °F	TC_4 °F	TC_5 °F	TC_6 °F	TC_7 °F	TC_8 °F	B_1 mils	B_2* mils	B_3 mils	B_4* mils	B_5 mils	S_1** μ in./in.	S_2 μ in./in.	S_3** μ in./in.	S_4** μ in./in.	S_5 μ in./in.	Q scfm	$\delta_{case\ front}$ mils	$\delta_{case\ rear}$ mils
LOWEST COLD HEEL GAP SETTING ~ 1.5 MILS																										
1	0	0	0	0	0	64	64	64	64	64	64	64	64	4.3	1.5	4.2	1.8	33.2	0	0	0	0	0	0	0	0
2	100	37	0.4	36	4.2	64	64	64	64	64	64	64	64	4.05	1.42	3.4	1.3	38.5	-4	-20	-7	0	-18	36.12	4	2.0
3	100	80.5	1.6	77	18	58	58	57	57	57	58	55	65	3.9	1.1	3.1	0.8	42.3	-12	-45	-10	2	-50	77.13	6.8	3.5
4	0	0	0	0	0	59	59	59	59	59	59	59	67	4.2	1.3	4.3	1.7	33.8	0	0	0	0	0	0	0.3	0.1
INCREASED COLD HEEL GAP SETTING ~ 3.5 MILS																										
5	0	0	0	0	0	62	62	62	62	62	62	62	62	6.35	3.35	6.6	3.5	33.4	0	0	0	0	0	0	0	0
6	100	35.5	0.5	34	6	62	62	62	62	62	62	59	64	4.6	1.7	4.6	1.6	39.0	0	-18	0	0	17	41.3	4.2	2.0
7	100	80	2.0	77	22	60	60	59	59	58	58	54	62	4.25	1.3	4.4	1.4	42.7	-5	-42	-2	-1	47	86.3	7.0	3.5
8	0	0	0	0	0	62	62	62	62	62	62	62	62	6.3	3.3	6.6	3.5	33.6	0	0	0	0	0	0	0.2	0.1
INCREASED COLD HEEL GAP SETTING ~ 5 MILS																										
9	0	0	0	0	0	67.5	67.5	67.5	67.5	67.5	67.5	67.5	67.5	7.4	5.0	8.15	4.9	35.7	0	0	0	0	0	0	0	0
10	SEAL FACES SEPARATE AT LOW P_2 – REPEAT TO ESTABLISH SEAL BEHAVIOR WHEN PARTING OCCURS																									
11	96	15	3	14	31	61	61	61	61	62	58	58	64	9.4	7.3	9.42	6.4	38.8	0	-20	-5	0	19	104.73	6.0	0.3
12	94	20	14.5	19	120	58	57	57	58	58	57	57	57	19.95	17.9	18.7	15.4	34.4	-2	-34	0	0	35	259	9.0	1.0
INCREASED COLD HEEL GAP SETTING TO ~ 8 MILS																										
13	0	0	0	0	0	67	67	67	67	67	67	67	67	10.6	8.0	10.5	8.25	33.4	0	0	0	0	0	0	–	–
14	100	12.5	4	11	40	57	57	57	57	57	57	57	62	9.8	7.4	9.5	7.35	36.1	-1	-31	-3	2	27	122	–	–
AT TEST POINT 14 FURTHER INCREASE IN PRESSURE CAUSES SEAL FACES TO SEPARATE																										

*Note B_2 and B_4 must be corrected to obtain true heel gap values. Also, unloaded heel gap settings are subject to the same corrections. See Appendix A.

**S_1, S_3, and S_4 are meridional, S_2 and S_5 are hoop stresses.

"J" Seal Test - Data Nomenclature

ΔP - Pressure difference across orifice out of tester (leakage)

P_1 - Pressure to orifice (inlet to system)

B_1 - Red - outer 9 o'clock

B_2 - White - inner 9 o'clock

B_3 - Green - outer 12 o'clock

B_4 - Black - inner 12 o'clock

B_5 - Runner motion w/r to casing

P_2 - Seal Cavity - Inlet Pressure

P_3 - Seal Cavity - Discharge Pressure

P_4 - Balance Piston Pressure

TC_1 - Correction Temp for Probes B_3 and B_4

TC_2 - Correction Temp for Probes B_1 and B_2

TC_3 - High Pressure Seal Cavity
TC_4 - High Pressure Seal Cavity } Hi-Press Inlet
TC_5 - High Pressure Seal Cavity

TC_6 - LP Seal Cavity
TC_7 - LP Seal Cavity } Seal Stator

TC_8 - Orifice Temp

REFERENCES

1. Smalley, A. J., Albrecht P. R. "Advanced Compressor Seal For Jet Engines"
   MTI 75-TR-59, November 1975. Prepared Under US Air Force Contract No. F33615-73-2043

2. Anon, "Fluid Meters", Part II, Sixth Edition, 1971 ASME, United Engineering Center 35 E. 47th Street, NYC, NY

☆ U. S. GOVERNMENT PRINTING OFFICE: 1977 — 757-001/541